RPN49

DEVELOPMENT OF AN ADVANCED X-RAY SOURCE

PIQR-226- and 227-1

April 1970

Prepared for

Defense Atomic Support Agency
Washington, D. C. 20505

Physics International Company
2700 Merced Street
San Leandro, California 94577

FOREWORD

This report presents the results (January 1, 1970, through April 1, 1970) of interim work on a program to develop an ultra-high-power (10^{12} watt) pulsed-electron accelerator and to utilize it as a bremsstrahlung source whose characteristics are beyond the present state of the art. The program is supported by DASA Contract No. 70-C-0063, and is monitored by Major R. Sullivan.

The goals of the program are not only to design, fabricate, and demonstrate a particular machine, but to provide the base of knowledge required to extend the technology to multi-megamp machines. These goals are being sought through a joint effort between members of the Nuclear Radiation Effects and Pulsed Power Departments of Physics International. The program is jointly supervised by I. Smith and G. Yonas with L. Hatch managing the development phase of the pulser and P. Spence managing the initial diode and beam studies. P. Champney, S. Shope and Kurt Nielsen are providing physicist support in the initial design and testing of switching, Mylar lines, and the tube. J. Benford, B. Ecker, and G. Loda are the physicists involved in diode investigations and beam transport experiments, with S. Putnam providing analytical support. The major design and fabrication tasks have been under the direction of R. Ryan and K. Beckman of the Engineering Department.

CONTENTS

ILLUSTRATIONS

ILLUSTRATIONS (cont.)

SECTION I

INTRODUCTION

A. PROGRAM OBJECTIVES

The goals of the program are to build and test a system that delivers a 50-kJ electron beam to a high Z target to create an intense X-ray source and to understand how, in the near future, X-ray sources 2 to 4 times as powerful may be achieved. The electron beam is characterized by a peak energy of 1 MeV with a pulse duration of 50 nsec, implying a peak current of 1 MA. Specific goals for the intensity and spatial extent of the X-ray source were presented in Physics International Proposal PIP-717.

The program is of 12-months duration. Of this period, approximately the first half is concerned with completing the design of the entire simulator system, procuring or fabricating the components, and testing the electrical pulse-generator portion, while work on the problems anticipated in the area of the X-ray tube is simultaneously performed using existing devices such as the low-voltage DASA Mylar line. The second half of the program is concentrated on using the generator in conjunction with the X-ray tube, which is then developed to the point of obtaining the highest X-ray output possible and on measuring and characterizing the X-rays. Experiments will be made to attempt to extrapolate the design of tubes with still larger radiation outputs and to investigate electron-beam transport as a means of combining the energy from several tubes.

B. CONCEPTUAL DESIGN

As described in PIP-717, the 50-kJ machine, which at the outset of the project was given the name Snark, will comprise two Mylar dielectric-line modules each of which delivers 0.5-MA peak current at

1 MV. The line modules are pulse charged together in a time of the order of a few microseconds and are switched simultaneously into a single X-ray tube.

To facilitate operation of the simulator at high voltage and high electrical stresses, each line module is designed to be rapidly and independently detached from the system for repair or replacement, and a spare is always available. Also, production of line modules is speeded up and electrical insulating properties are improved by assembling each one in air, evacuating it, and vacuum impregnating with the aqueous solution used as an operating medium to suppress flashover.

More line modules can, if required, be operated together in this way, providing much larger sources of energy. However, using more than two is outside the scope of the present effort. Indeed, the efficient use of much larger quantities of energy may require a number of tubes whose electron beams are transported to a common target--probably in a linear magnetic pinch--implying a limit to the number of line modules that would be needed to feed each tube.

The design of the Marx and its high-voltage feed to the line modules is relatively straightforward. That of the line modules themselves and their associated switching currents follows work performed by PI under previous DASA contracts and utilizes developments in J. C. Martin's group at AWRE, Aldermaston, UK; it is discussed in some detail in PIP-717. The most fundamental advances required in this program are associated with the area of the tube, and in particular with the diode and the electron beam. The starting point here will be experience gained with other high-current systems such as the 730 Pulserad, the low-impedance SAMSO facility, and the DASA low-voltage Mylar line. These diodes have been developed to handle energies up to 20 kJ and are routinely used in conjunction with special sample-protection methods to irradiate test objects.

C. GENERAL STATUS

The most critical activity during the first quarter has been the detailed design, procurement, and fabrication of the necessary hardware. This effort has closely coincided with the required schedule and the assembly of the first Snark line module can begin in only a few weeks.

Developmental testing of especially important regions of the line module has been conducted simultaneously and is expected to continue for a number of weeks. Supporting work on diodes (on the DASA low-voltage line) and on electron-beam propagation (on the 730 Pulserad) is underway.

Section II of this report outlines the processes followed in designing the Snark hardware, describes the final designs, and presents the status of procurement and fabrication. In Section III the results of experimental effort in the various areas are described. An up-to-date schedule, program plan and summary of financial status are presented in Section IV.

SECTION II

DESCRIPTION OF COMPONENTS AND STATUS

A. VACUUM IMPREGNATION SYSTEM

In the present modular design, the highest practical charging voltage will be employed. In order to have a reasonable module life time, all air bubbles must be excluded from the copper sulphate immersion medium. In the past at PI, the Mylar lines have been assembled in the copper sulphate solution, with the resulting inconveniences and the possibility of including or subsequently generating air bubbles. It is expected, based on past experience with high-voltage transformers, that vacuum impregnation will eliminate these risks. A system to vacuum-impregnate the Mylar Blumleins with water loaded with copper-sulphate solution has been designed to facilitate the assembly of high-quality, long-life-time line modules.

The impregnation system consists of a large vacuum tank to hold the Mylar line tray and a vacuum chamber to contain the copper sulphate solution while it is being degassed. The Mylar line is pre-assembled dry in the tray. The tray is slid into the impregnation tank and the tank is then evacuated to the base pressure of the system (a procedure that will probably take a day or two) thus excluding the air from the layers of Mylar and copper. When the above cycle is near completion the copper-sulphate degassing tank is filled with water from a commercial deionizer unit and concentrated copper sulphate solution is added to bring the solution to the desired resistivity. A water-seal vacuum pump, designed to pump directly on fluids without cold traps, is used to remove the air from the water. A stirring system is incorporated to prevent the water from freezing while it is being degassed. A remote sensing head is used in the solution to measure the resistivity.

The solution is transferred through a transfer line to the impregnation tank below the degassing tank under the weight of the solution. The level in the trays can be viewed through ports in the impregnation tank. The tray is filled to a level well above the stacked Mylar line. The system is then brought slowly up to atmospheric pressure to allow the solution time to flow uniformly between the many layers of Mylar and copper. The fabricated system is shown in Figure 1. The impregnation tank has a capacity of 8 ft by 2 ft by 20 ft to accommodate a single module tray. The interior of the tanks must be resistant to corrosion by the water and copper sulphate solution. Also the tanks must be constructed as vacuum vessels. Stainless-steel construction was contemplated but was discarded as prohibitively expensive. Instead painted steel has been used throughout. The inside surfaces have been primed and finish-coated with polyurethane paint. This substance is resistive to flaking under vacuum and to decomposition in the copper sulphate solution.

At one end of the impregnation tank is a door through which the trays enter the vessel. A hatch at the opposite end is used for access to the enclosed end of the tank for maintenance and ventilation. The tray rolls on its own grooved wheels along a stainless-steel track inside the tank. View ports are placed in the top of the tank; the general condition of the trays including the fluid level can be seen while they are in the tank.

The degassing tank rests atop the impregnation tank and the two are connected by a transfer line inside the lower tank. A plastic tube is attached to the transfer line so that the solution can be directed into the tray. The water level in the degassing tank is measured with a sight level and the condition of the surface of the water can be viewed through ports in the top of the tank. Access to the inside of the tank is through a hatch in the top.

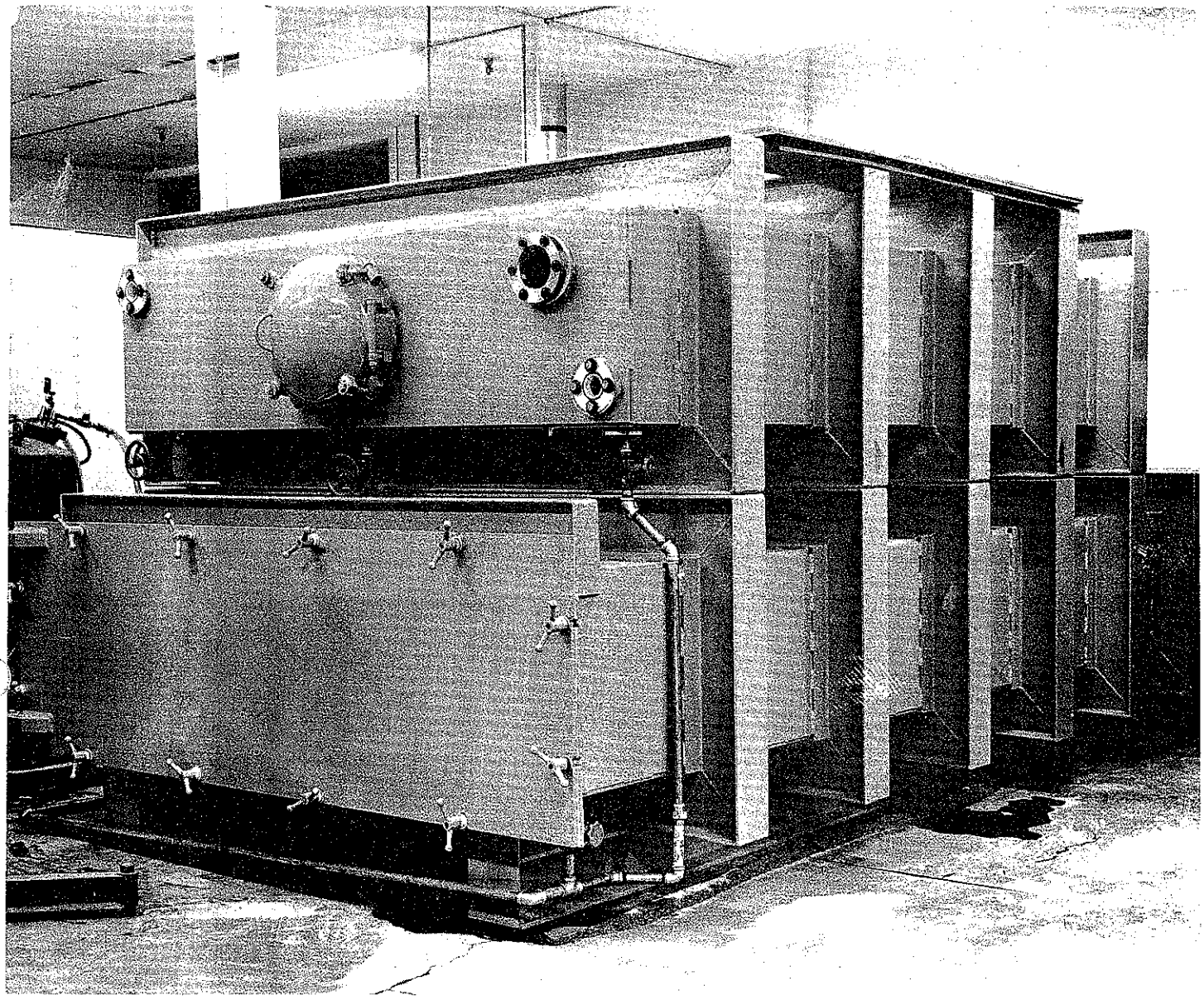

FIGURE 1. MYLAR IMPREGNATION TANK

The vacuum-system plumbing is constructed from stainless-steel tubing and valves to avoid corrosion from the copper-sulphate solution. Two pumps have been incorporated in the design--a large capacity oil mechanical pump (STOKES) and a large capacity water-seal mechanical pump (SIHI). The former will be used with a cold trap whenever water vapor is present in the system. When a completely dry tray is being impregnated, the STOKES can be used without the cold trap. It is planned to use the SIHI to degas the water in the upper tank and to use either the STOKES or SIHI to evacuate the tray and impregnation tank, depending on the amount of water present in the tray.

The tanks have been leak-checked and the vacuum system is being completed. The system will be ready for a test vacuum impregnation by the end of April.

B. MODULE

The maximum charging voltage for reliable operation of Mylar Blumleins to date is in the region of 500 kV. Hence, to attain 1-MV output under matched conditions, it is necessary to operate two Blumleins in series. Because of the flat line design of the Mylar Blumlein, it is easy to stack several lines forming a series parallel combination (which will be referred to as a line module). A line module formed in this way has the added feature that the high-voltage electrode is buried for the majority of its length in the middle of the module, thereby reducing insulation problems and line-gain losses from the high-voltage electrode coupling through the water to ground(Figure 2).

With regard to the 1-MA current requirement, the limitation is in the line current density available from the Mylar dielectric charged to a given electric field. The width of the line is limited

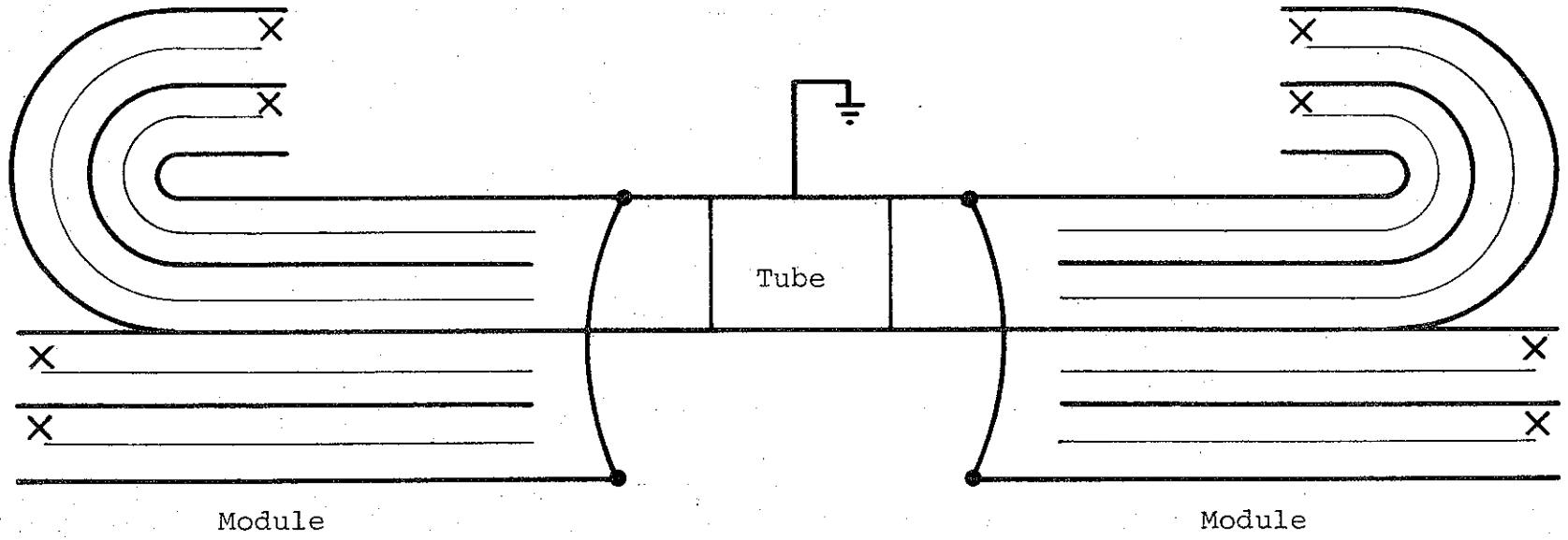

FIGURE 2. SCHEMATIC OF MYLAR MACHINE

by the maximum-width Mylar available, which is 6 ft; thus the electrode of the line can be only 4.5 ft wide. Hence, each line module is only capable of carrying just over 0.5 MA and two modules are required to attain 1 MA.

Each module is composed of 120 sheets of 0.010-in. Mylar 6-ft wide, about 18 ft long and 9 sheets of copper 0.010 thick, 4-1/2 ft wide. It has been found experimentally that a 25-mil radius at the edge of the copper electrodes forming the lines is adequate in combination with conduction in the water to prevent edge breakdown. To save the cost of 50-mil-thick copper, the edge of the 0.010-in. copper is rolled up in such a way that a 50-mil bead is formed around the line. Layers of precut and shaped Mylar and copper are assembled in the line module tray. The line module tray is then transported to the impregnation system on a cart and the tray is then transported to the impregnation system on rails. The line module is then impregnated with degassed water of the correct resistivity while under vacuum. The vacuum impregnation greatly facilitates the line module preparation since all the cutting and stacking of materials can be done in air. Simple repair work can of course be undertaken while the water remains in the tray, but for more complicated repair work the line module would be pulled away from the tube, a spare substituted, and the damaged line module repaired after the water had been drained.

Each Blumlein has an impedance of 1.25 Ω; hence the series parallel combination, namely the line module, has an output impedance of 1.25 Ω, with each Blumlein charged to 500 kV. The output per module into a 2-Ω load is approximately 1.23 mV, 610 kA. The length of the module is chosen to give a pulse duration of 50 nsec and the energy stored in each module at 500 kV is about 40 kJ.

The top series Blumleins of the module are folded back so that the switch box is accessible for loading and the lug, which must be connected to the charged electrodes, will not be exposed (see Figure 3).

The triggering of the individual slave switches in the Blumleins from a common master switch can be accomplished in a number of ways. One way is to feed the trigger pulse by way of high-voltage coaxial cables to each switch and connect the cable between the trigger lead and switch box of each Blumlein. This results in the braid of two cables rising to 500 kV and the other two cables to 1 MV for the duration of the output pulse. This voltage can be isolated by winding the trigger cables into inductances. It may also be possible to rely upon the braids of the trigger cables to form the earth connections during the charging phase, provided, of course, that the charging leads are brought in side by side with the trigger cables to minimize the inductance of the charging circuit.

The trigger cables will also have series resistors positioned at the switch end to reduce the amplitude of the transients fed back down the cable due to the switch firing. This method has proved very satisfactory with the lines tested to date (see Figure 4).

No detrimental effects have been observed as yet as a result of feeding the current asymmetrically from the lines to the tube on either the 0.1 Ω or the 0.3 Ω Mylar generators. However, with these systems the line width has been greater than the tube diameter. In the case of Snark the tube diameter is about 5 ft and the line width 4-1/2 ft and it is for this reason that the bottom series Blumleins will be paralleled into the tube in such a way as to make the current distribution into the tube more symmetrical (Figure 5).

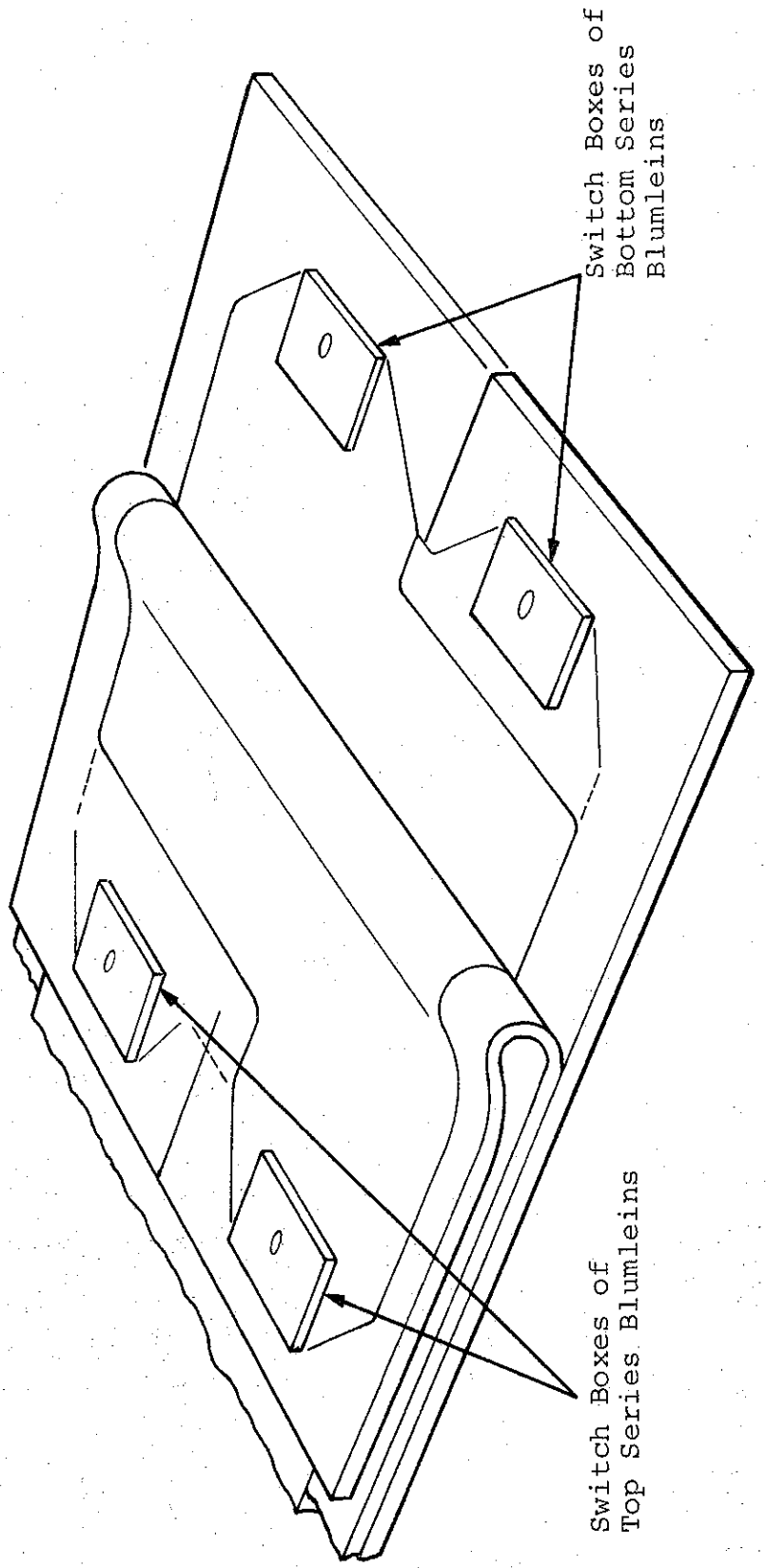

FIGURE 3. SWITCH END OF MODULE INDICATING SWITCH LAYOUT

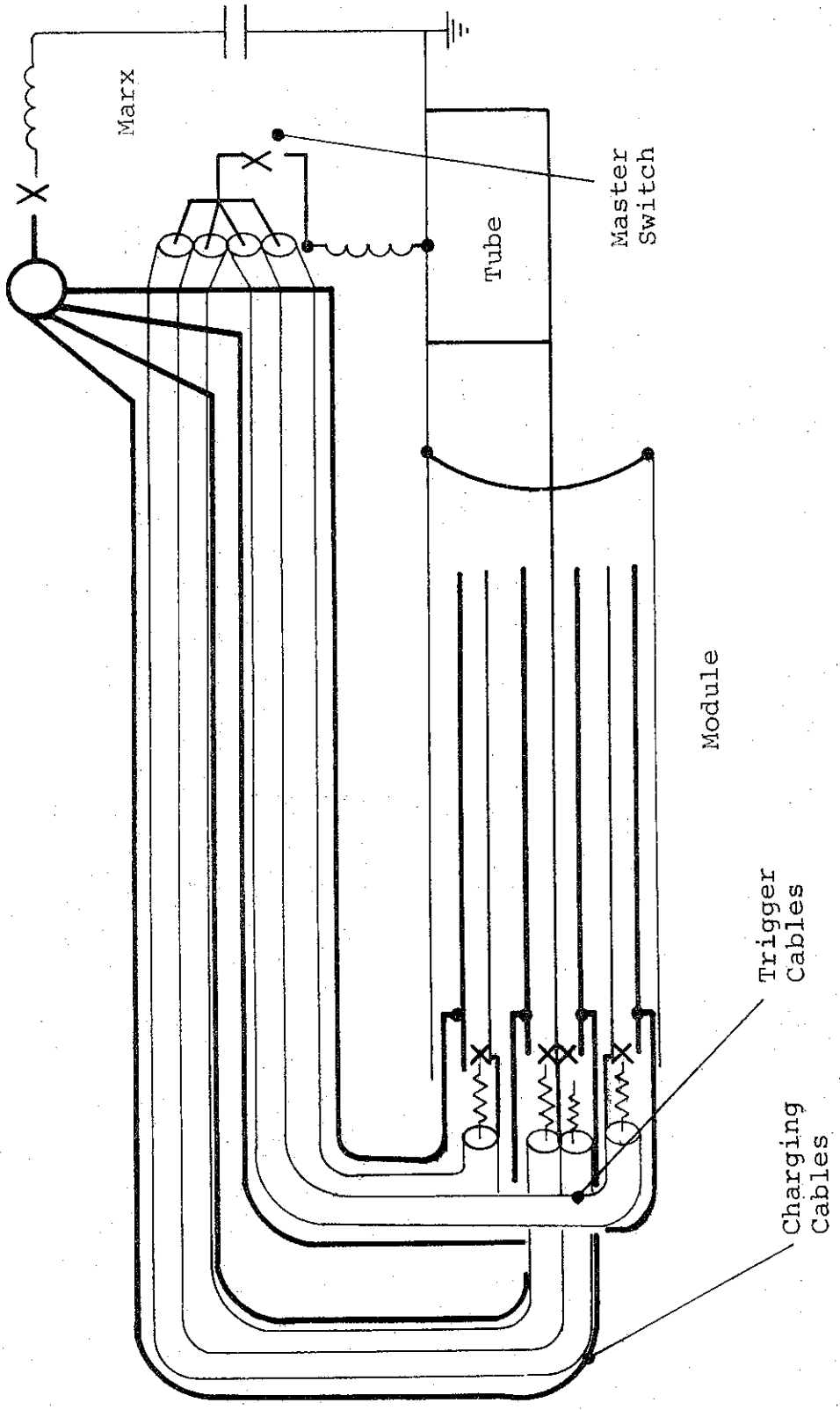

FIGURE 4. CHARGING AND TRIGGERING OF MODULE

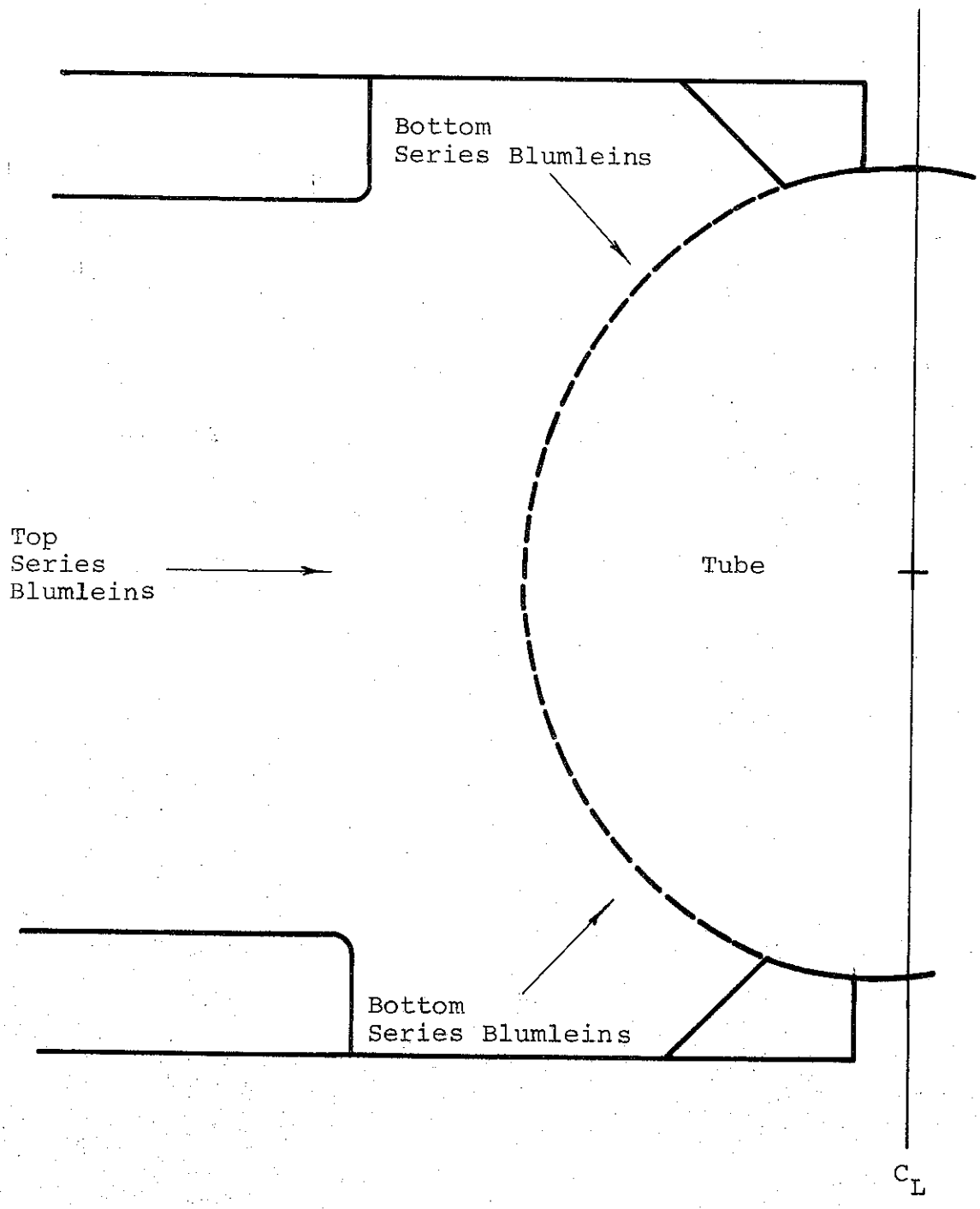

FIGURE 5. OUTPUT END OF MODULE

C. TUBE AND EXPERIMENT CHAMBER

A tube capable of conducting a megamp for short times (50 nsec) at 1 MV accelerating voltage must have very low inductance if it is expected to reach peak voltage during the pulse length. With an e-folding time of greater than 20 nsec, the maximum voltage realized during the pulse would be inductive-limited to less than 90% of peak line voltage. The tube has been designed to keep the risetime less than 20 nsec.

The main design requirements of the tube are as follows:

1. Low inductance
2. Insulation against 1 MV
3. Ease of attachment to the Mylar lines
4. Ease of assembly and disassembly to clean tube
5. Minimum distortion of the wave entering the tube from the Mylar lines
6. Ease of attaching diagnostic devices to the diode
7. Stability of the anode-cathode plate distance when under vacuum
8. Insulation of the tube from the surrounding metal electrical ground surfaces (i.e., support tank)

To minimize the inductance, the height of the insulator and the cathode plate-anode plate distances were made as small as possible, while the diameter of the insulator was made as large as conveniently possible. The result is an insulator 6 in. thick and about 5 ft in diameter. This insulator should be capable of standing off over 1.5 MV. The cathode plate-anode plate distance is 2 cm. The well-oiled, smooth parallel surfaces will, as a result, be operating in a

field of 500 kV/cm in vacuum. Both the anode plate and the cathode are rigidly braced with ribs to reduce any deflection to less than 1 mm when the tube is under vacuum.

To design the vacuum insulator interface, the potential lines across the interface were plotted using various geometries of the anode plate, cathode plate, and Mylar-line tube-coupling piece. The accepted design was that which gave the most uniform voltage grading across the interface and which gave minimum wave distortion. The electric field makes the same angle with the interface that occurs at the interface of a normal 45-degree insulator between two parallel plates with 6-in. separation.

The tube is built up in the following way (see Figure 6): the insulator is placed on top of the cathode plate; the water barrier forming part of the anode structure is placed on top of the insulator; and the three components are bolted together with nylon rods.

The cathode plate which is at high voltage must be insulated from the support tank. An epoxy casting is used to insulate the tube. The casting and the lower side of the cathode plate are immersed in copper-sulphate solution so that the inside of the cathode plate and casting need not be smooth. However, the presence of the copper-sulphate solution clamps the voltage across the insulator and constitutes a capacitive loading in parallel with the tube. A 3-in. thickness of the epoxy casting has been chosen to reduce this capacity to less than a nanofarad, thereby robbing the tube of less than a few percent of the energy.

The removable part of the tube is made up of the anode plate, vacuum system, and the experiment chamber. The anode plate has a removable section about 2-ft in diameter in which diagnostic devices and the X-ray target are held. The diagnostics to be used will be

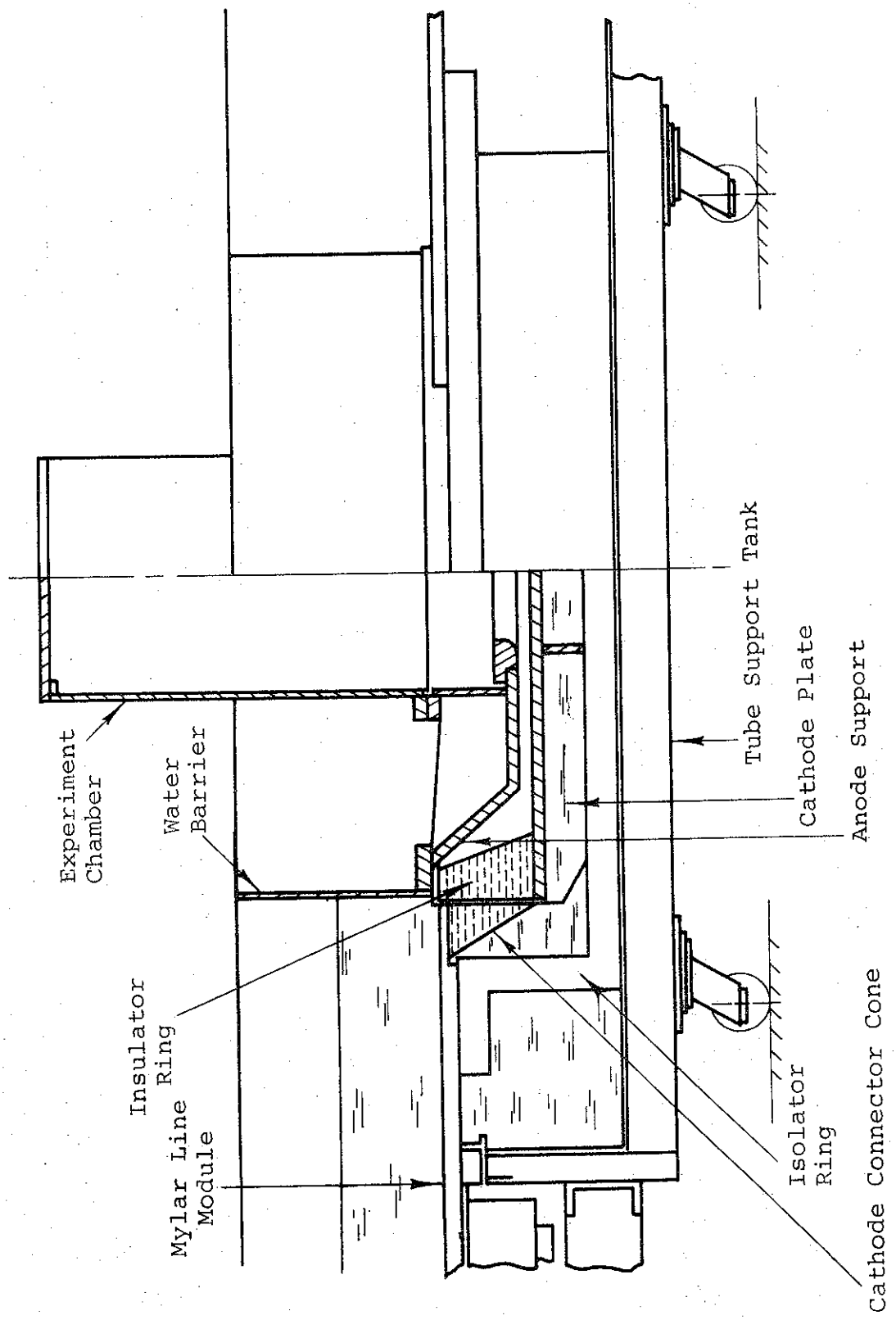

FIGURE 6. TUBE ASSEMBLY

decided after completion of the tests on the low-voltage line. An anode holder will incorporate a means of remotely varying the anode-target-cathode distance while the tube is under vacuum.

During each shot, the thin anode target ruptures and debris is scattered throughout the tube and experiment chamber, which requires the tube to be cleaned after each shot. The tube separates so that the anode plate, vacuum system, and experiment chamber lifts off. The insulator can then be inspected and cleaned. All tube surfaces can be re-oiled. The experiment chamber can then be reloaded and a new anode target put in place. The removable section can be replaced and the tube evacuated.

The experiment chamber is attached to the anode plate by way of a transition piece that contains the vacuum connections for the experiment chamber. The experiment-chamber lateral surfaces have been kept free of any feed-throughs or ports so that a cap of lead can be dropped over the chamber for radiation shielding. Vacuum connections are made for the tube through the anode plate.

The anode plate, cathode plate, water barrier, insulator, and epoxy casting are finished and are in-house. The experiment chamber, vacuum system, and line coupling piece are being fabricated. The target holder and diagnostics are being designed. The tube support tank is completed.

By mid-May, the tube will be assembled and vacuum tested without the experiment chamber, using a 2-ft blank off plate for the diagnostics section.

D. MARX GENERATOR

The Marx generator has been designed and is being fabricated. A surplus Marx tank will be used to make a very compact generator. The design uses the 0.5-μF, 100 kV Aerovox capacitors and oil from the Aurora Test Facilities at PI.

Each line module has an input capacitance of about 0.3 μF. The two modules will have a total of 0.6 μF. For efficient energy transfer from Marx to modules, the Marx has been designed to have an output capacitance slightly greater than 0.6 μF. Also, to provide efficient energy transfer when only one module is being charged, the Marx has been designed to be convertible to half the output capacitance by using only half of each stage.

The individual stages are plus-minus charged to ± 45 kV. Each stage has 12 capacitors in two stacks of six with their terminals tied together. The stored energy in each stage is 27-kJ at 90-kV charge voltage and capacitance of 6 μF. Each stack can be halved quite easily to convert to 13.5 kJ per stage at 90-kV charge voltage and 3 μF per stage.

With six stages, the stored energy in the Marx is 160 kJ at 90-kV charge voltage. This charges two modules to over 500 kV. Additional stages can be added if needed to raise the stored energy to nearly 250 kJ.

SECTION III

PRELIMINARY MACHINE TESTS AND BEAM STUDIES

A. SNARK RESEARCH

Prior to line-module fabrication, research has been directed towards the following:

1. Development of a reliable switch for the Blumlein
2. Controlling dielectric breakdown from high-speed transients by adjusting the edge grading on the lines
3. Investigation of the causes of line-gain loss

Items 1 and 2 have been carried out at full line voltage (above 500 kV) while Item 3 has been performed on a scaled-down model line.

1. Switch Design

Location of the switches in previous Mylar lines has been achieved by positioning the required thickness of pre-stabbed polyethylene in between the Mylar sheets, contact being made to the line electrodes by means of holes cut in the Mylar sheets and by the use of aluminum discs (Figure 7). There are a number of disadvantages to these arrangements, some of which were not obvious before prolonged use. These disadvantages are summarized below:

1. The design cannot be used economically at 500 kV because a special switch card needs to be prepared. For an operating voltage of 500 kV, about 3/8-in. polyethylene is required and the gradient existing in the water at the edge of the polyethylene card would be sufficient to exceed the breakdown strength of the water and the resulting streamers would puncture through the Mylar. The gradient could be reduced to safe level by tapering the edges of the polyethylene, which greatly increases the cost of the switches.

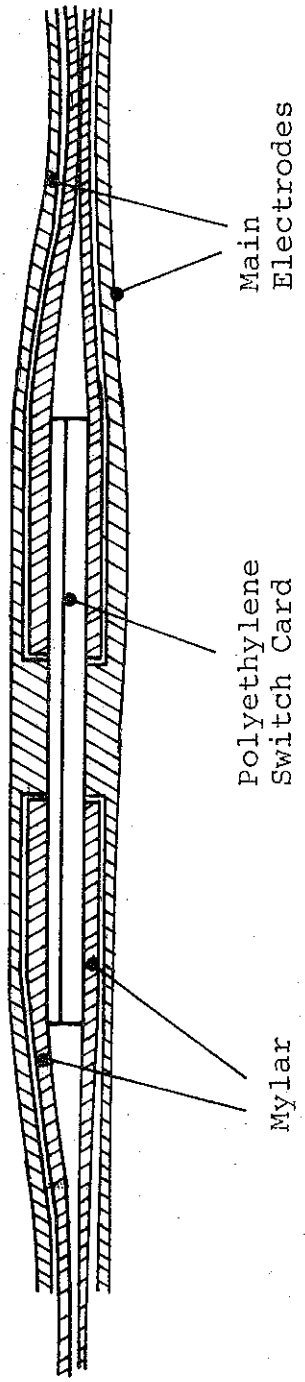

FIGURE 7. PREVIOUS SWITCH DESIGN

2. The method of inserting and removing the switches leads to damage to the Mylar sheets. The continual folding of the sheets of Mylar to enable the introduction of the polyethylene switch card and the process of removing bubbles and debris causes the Mylar to become scratched and creased. This condition eventually weakens the Mylar so that it becomes vulnerable to electrical breakdown.

3. The polyethylene cards must be smooth or else bubbles will appear in the feather edges. To prevent this requires additional costly and time-consuming hand finishing of the edges to avoid electrical breakdown due to the presence of bubbles.

4. When the switch fires, energy is dissipated in the electrodes and gases are formed. As a result the electrodes tend to become distorted and bubbles are driven in between the sheets of Mylar. The bubbles must then be removed by hand before the next shot. The distortion in the electrode leads to poor switch-electrode contact and eventually requires the switch site to be rebuilt.

To avoid some of these long-term difficulties and at the same time speed up operation, a new type of switch was designed. Pre-stabbed polyethylene is still used but this design (see Figure 8) goes a long way toward eliminating the problems described above.

The pre-stabbed polyethylene slides into a sturdy, stainless-steel box, the bottom face of which has a hole cut in it that exposes the stabs in the polyethylene to the line voltage by a heavy lug connecting through the Mylar to the other line. The lug has a lip on it to locate the sheets of Mylar and prevent bubbles from being introduced in between them. Flashover between lug and box is prevented by resistive grading in the water. Since the edges of the polyethylene are shielded by the box, no special edge preparation is

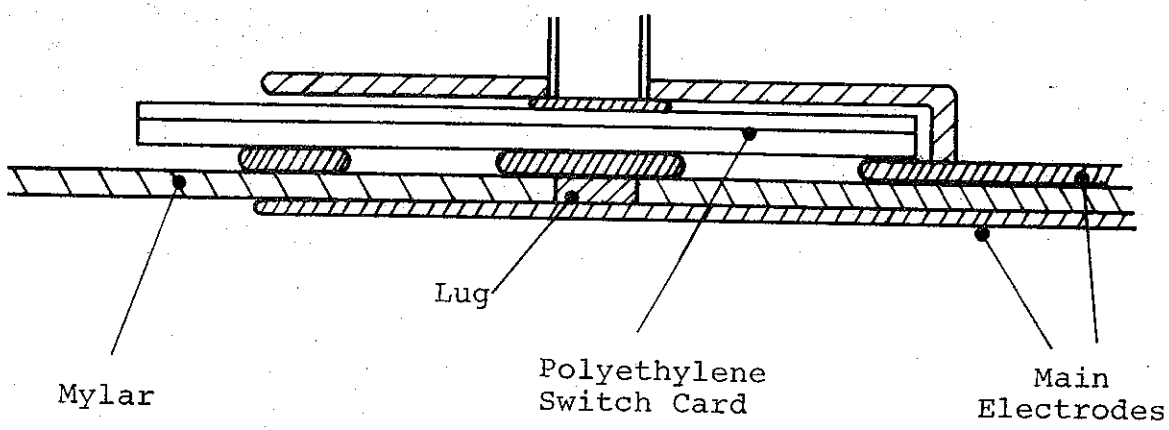

FIGURE 8. NEW SWITCH DESIGN

required. The switch boxes are located on top of the lines eliminating the need to continually bend or handle the Mylar. The boxes can be attached to the line electrode conveniently.

With this design, the switch region is made mechanically very strong. Hopefully, this design will enable not only greater reliability, but a much faster turn-around time in terms of loading switches.

The new switch design has been tested at over 500 kV in a Blumlein with the final Snark thickness of Mylar and found to work very well. The self-breakdown voltage of the stabbed polyethylene cards has been checked against the depth of the stab using the new switch. The curves for 1/4-in. and 1/8-in. polyethylene are shown in Figure 9. As an example of its use, in order to charge the lines to 500 kV and trigger the switch card, the self-break of the card should be in the region of 720 kV, which means that the switch card is triggered at 70% of self-break--a level that has proved to be safe in the past. If the switch card is made up of a 1/4-in. and 1/8-in. card of polyethylene, with the trigger strip positioned in between the cards, then it requires that the 1/4-in. and 1/8-in. polyethylene cards self-break at about 475 kV and 240 kV, respectively. It can be seen from Figure 9 that this requires a 10.5-mil stab in the 1/4-in. card and an 11-mil stab in the 1/8-in. card. A table (Figure 10) can be drawn up indicating how the polyethylene cards should be stabbed for a given line voltage.

2. Line Tests

Tests have been conducted to investigate the electrical breakdown that can occur at the edge of the lines due to high-speed voltage transients. The logic was to operate a model line where edge breakdown would occur and then adjust the line-module parameters to eliminate the effect at the design voltage of Snark. The edge breakdown can be

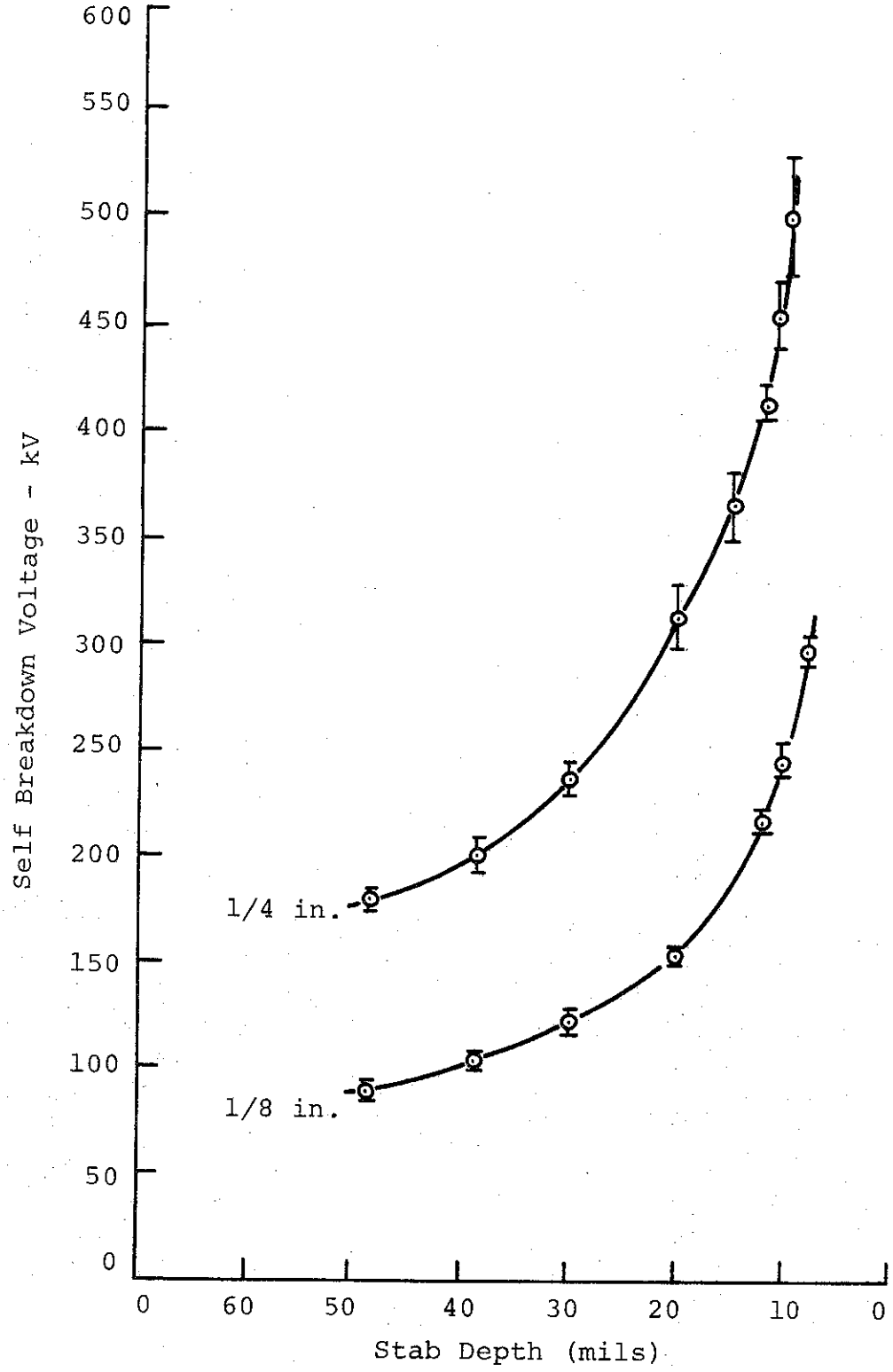

FIGURE 9. CALIBRATION CURVES FOR POLYETHELENE SWITCHES (ERROR BARS INDICATE ONE STANDARD DEVIATION)

V Line kV	MASTER SWITCH TRIGGER V/3	Stab 1/8-in.	70% SAFETY V Total SB* kV	SLAVE SWITCH V 1/4-in. SB* kV	Stab 1/4-in.	V 1/8-in. SB* kV	Stab 1/8-in.
100	33		143	95		48	
150	50		215	142		73	
200	66		286	191	42	95	46
250	83		357	237	30	120	31
300	100	42	429	286	23	143	23
350	116	34	500	334	18	166	18
400	134	26	572	382	14	190	14
450	150	21	642	427	11	215	12
500	167	18	715	477	10½	238	11

*SB - Self Break

STAB (mils)

FIGURE 10. SWITCH CARD DATA FOR A GIVEN LINE VOLTAGE

eliminated by both decreasing the resistivity of the $CuSO_4$ solution and by increasing the thickness of the copper electrode. Both techniques increase the voltage-edge grading distance, thus prohibiting large voltage gradients, which cause electrical breakdown, from developing across the Mylar at the edges of the copper. Experience on the 0.3 Ω DASA Mylar line predicted a grading distance at which breakdown would occur on the Snark line. Since it is easiest to change the resistivity of the copper-sulphate solution while the edge thickness is more difficult to change, it was decided to keep the edge thickness constant and vary the resistivity.

A line was constructed with the same insulation as the Snark lines, i.e., 15 sheets of 0.010-in. Mylar. Since the grading is not dependent on the width of the line, and to conserve Mylar, the width of the line was made 1 ft. The reduced width leads to a higher impedance and hence to a faster rising output pulse. Because the high-speed transient grading is made more difficult by a faster risetime and is not significantly effected by increasing the pulse length, a 20-nsec line was used rather than the 50-nsec Snark pulse length. This faster risetime makes the grading more critical and leads to a conservative solution to the edge design.

The line edging was made the same as the (0.3 Ω) DASA Mylar line and the resistivity set at 8 kΩ-cm. Edge breakdown occurred as low as 400 kV although some shots were fired as high as 500 kV without damage. The resistivity was reduced in steps until 2 kΩ-cm, where no further edge breaks occurred at charging voltages up to 600 kV. As will be shown in the next section, this value of resistivity is still above the level at which line-gain losses due to excessive grading will be significant.

The previous tests were conducted using self-break stabbed switches in the Blumlein. The next step was to trigger the switches to establish a triggering scheme in preparation for triggering Blumleins from a master switch.

A double Blumlein has been constructed and the two lines have been switched successfully. These tests are continuing and have thus far not required any change to be made to the original design of the final line module.

3. Generator Gain Studies

While the full-voltage line tests were being conducted, a series of scaled-down model tests were conducted with a single Blumlein. The object of these experiments was to determine the effects of very low resistivities and large electrode thicknesses upon the Blumlein gain, under short circuit, matched, and open circuit conditions, so that we might understand more fully the implications of changing these parameters on the final module.

The line insulation was one sheet of 0.01-in. Mylar. The electrodes were 6 in. wide and 14 ft long. Switching was done by a single self-breaking solid-dielectric switch operating at 20 kV. The line was constructed so that the edge radius could easily be changed by adding folded copper strips, in addition to changing the copper sulphate resistivity.

At the time of this writing the results of these tests are being analyzed and will be fully reported in the next progress report. The initial conclusions are that the Snark machine may have gain losses of the order of a few percent.

4. Remaining Work

Although it is intended to fabricate the first complete line module in the next few weeks, experiments will continue at full voltage on reduced-width lines to study the interaction between the series-parallel Blumleins with respect to edge grading and line gain. Various methods of triggering the individual Blumleins will be checked with the emphasis on reducing the transients that result when the switches are fired. These transients can lead to trigger cable breakdown if they are not minimized by selecting the proper cable routing and isolation.

B. HIGH ν/γ BEAM GENERATION AND PROPAGATION

1. Introduction

The major goals of this portion of the program relate to development of diode diagnostics and design, high ν/γ electron beam handling techniques, and high ν/γ beam transport techniques for direct application to operation of Snark (1 MeV, 1 MA) and future higher-current machines.

High ν/γ beam work performed for DASA during the past two years using primarily the 250 keV, 200 kA beam from the 730 Pulserad has resulted in development of techniques for generation and control of high current beams, documentation of beam-plasma interactions which "regulate" beam characteristics and beam-loss mechanisms, and identification of problem areas in extension of these techniques to even higher ν/γ conditions. The beam work conducted to date has been directed toward solutions to the problem areas in efficient generation and propagation of very high ν/γ beams.

Operation of Snark as a high intensity pulsed γ source will presumably encompass both extended and point source geometries. Extended source operation should provide a uniform large area γ flux, beginning with an extended uniform-flux electron beam, while point-source operation should attempt to concentrate the electron beam into as small an area as possible. Two considerations for implementation of these geometries are control of beam current density at the converter location and containment of the converter explosion.

For extended source operation it is desirable to prevent beam pinching in the anode-cathode region so that the converter can be placed at the anode plane. If current densities are low enough, the converter explosion will not damage the diode and low atomic number absorbers can be used to prevent converter debris from entering the target chamber. Decreases in current densities at the anode have been shown to be feasible by using multiple, magnetically isolated cathodes (Reference 1), and recent work with hollow annular cathodes also shows this to be a promising approach.

It is possible that point-source operation will be hampered if the converter is placed at the anode because of converter debris contamination or even damage of the tube. In this case it will then be necessary to efficiently transport the beam away from the anode and concentrate it at a distant converter location. Past work with beam propagation in initially non-ionized low-pressure gases has shown this approach to beam transport to be inefficient, even at $\nu/\gamma \simeq 10$, due to poor containment of high electron transverse energy components and back emf generated by the rapidly increasing beam current. Our approach to the solution of the beam transport problem is currently directed at beam propagation in a pre-ionized low-pressure gas with the magnetic field generated by a linear pinch discharge to contain the high transverse energy components. Work is now proceeding in two areas: diode studies and development of diagnostics (Section III, B, 2), and the linear-pinch discharge (Section III, B, 3).

The most important application of beam transport will follow if multiple cathodes are required in connection with Snark. In this case, beam transport and combining at the converter will be carried out. Finally, it is likely that any multi-megampere machines of the future will require multiple tubes to avoid inductance problems, and beam transport will be essential.

2. Diode Study and Diagnosis, 0.3Ω Line

Past work has shown that diode operation becomes strongly affected by beam self-magnetic fields as ν/γ is increased. For purposes of application to Snark, the existing DASA 0.3Ω Mylar line (hereafter designated as DML) was chosen for initial diode studies since ν/γ for this machine is very close to that expected for Snark.

Generator	Mean Voltage	Peak Current	$\nu/\gamma = \frac{I\ (amps)}{17{,}000\ \beta\gamma}$
738 Pulserad	250 kV	200 kA	12
DML	120 kV	300 kA	24
Snark (design values)	1 MV	1 MA	21

The first goal was development of a diode diagnostics package (voltage and current monitors) for use in studies of low inductance tubes used with strip-line generators. An annular capacitive voltage monitor was designed and tested and is described in this section. Current diagnosis employed techniques already developed under past DASA beam programs (self-integrating Rogowski coils and Faraday cups).

Results of diode studies to date are also given in this section. Evidence of diode impedance collapse during the pulse (observed before with high ν/γ diodes) is consistent with the following interpretation: impedance collapse appears to be a direct result of anode explosion during the pulse, resulting in a decrease in anode-cathode gap. The impedance is in agreement with the Child's law prediction (using the constant k = 136) and an anode material velocity of $\approx$ 1.5 cm/μsec. Allowance for this anode explosion is important in the prediction of operating characteristics of low-impedance diodes, since it can affect output voltage, current, and pulse duration.

a. Diagnostics

1. Voltage Monitor

Due to the large dI/dt characteristic of the machine, the voltage must be sampled very near the diode. If this is not done, the monitor will read both the true A-K voltage plus a large L dI/dt component. Monitoring outputs placed on the Blumlein feeding the tube have little relation to the actual voltage at the diode. This problem was solved by constructing a capacitive monitor in the anode plate of the tube in close proximity to the diode region, thus minimizing the inductive portion of monitored voltage.

The electrical schematic of the monitor is shown below.

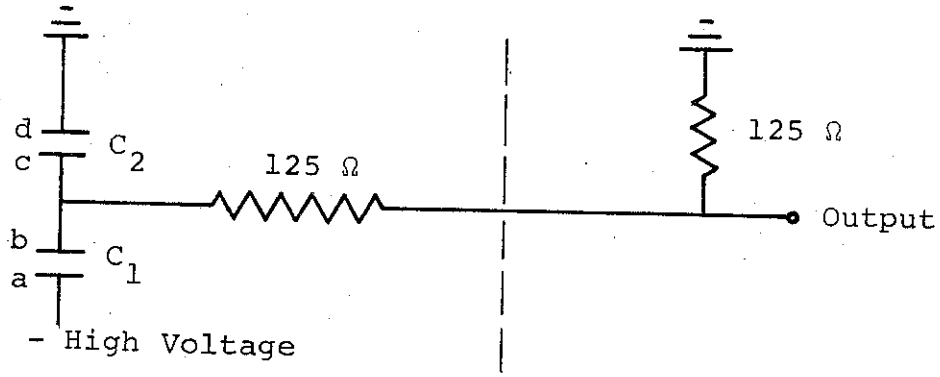

The labels on the capacitor plates correspond to those shown on the actual pieces in Figure 11. In situ calibration gave an attenuation ratio of 365:1 implying values of C = 3.5 nF and C_2 = 9.5 pF. This monitor has a limited readtime due to the finite value of the oscilloscope impedance. With a 125Ω resistor in series with the 125Ω cable (inputs directly to a 125Ω Tektronix 519), the R = 250Ω gives a t = RC ≈ 880 nsec which is sufficiently long for our 50-60 nsec pulses. This extra 125Ω resistor adds an extra x2 attenuation to the system.

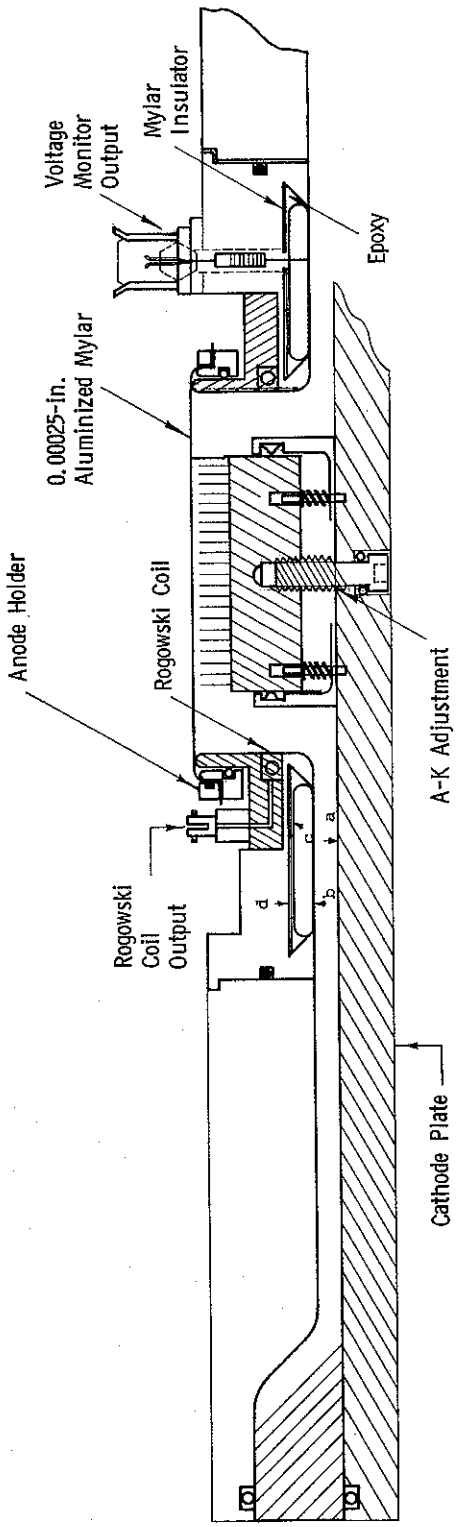

FIGURE 11. LOW-INDUCTANCE DIODE AND DIAGNOSTICS

A monitor of this type has been in use for the last three months, giving excellent service. Output traces are shown in Figure 12. Oscillatory structure (see Figure 12b) at the end of the pulse (when the diode shorts out) seems to be due to a growing plasma emanating from the diode region and effectively increasing the value of C_1 and hence lowering the division ratio. Scintillator photodiode records show a pulse duration consistent with the duration of the capacitive voltage monitor pulse, indicating diode shorting at this time.

Due to the diode inductance existing between the voltage monitor location and the cathode needle tips (and any stray inductance in the monitor circuit itself), the monitor output includes a small inductive component proportional to dI/dt. This inductive component has been measured by shorting the anode-cathode gap ($V_{A-K} \equiv 0$) and correlating the monitor output with dI/dt. For shots with finite A-K gaps, the inductive component was deduced from the relation

$$V_{inductive} = \frac{dI}{dt}\left[\frac{V_{inductive\ (A-K\ =\ 0)}}{\frac{dI}{dt}\quad (A-K\ =\ 0)}\right]$$

The correction to voltage monitor outputs for typical shots near 120 kV averages less than 15 percent. Figure 12c shows an estimate of inductive component for the shot pictured in Figure 12a and b.

It is interesting to note that if the inductive component is purely due to the diode inductance (i.e., no contribution from the monitor circuit), the empirical measurement

$$V_{inductive\ (A-K\ =\ 0)} = \frac{7.5\ KV}{KA/nsec} \cdot \frac{dI}{dt}$$

a.

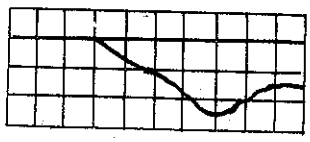

Diode Rogowski Coil
185 kA/div
20 nsec/div

b.

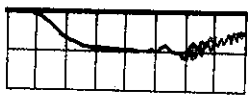

Capacitive Voltage Monitor
131 kV/div
20 nsec/div

c.

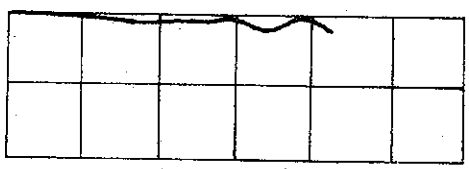

Scaled Inductive Pickup
of Voltage Monitor
131 kV/div
20 nsec/div

FIGURE 12. DIODE DIAGNOSTIC TRACES

indicates a diode inductance of 7.5 nH. A calculation of expected inductance based on the following dimensions yields L ≈ 6 nH in reasonable agreement with the measurement.

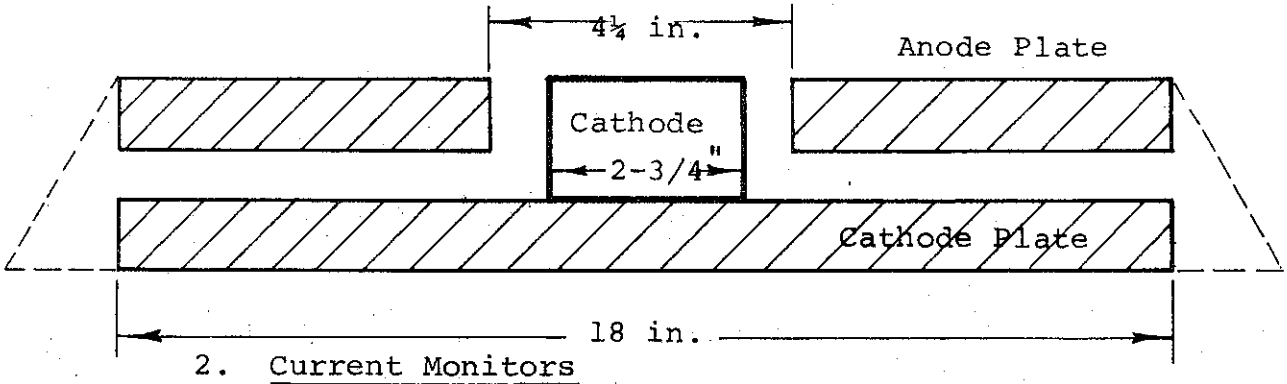

2. Current Monitors

Three current diagnostics are now in use on the line. The propagated net current and propagated primary current diagnostics are the Rogowski coil and Faraday cup described in DASA Reports 2175 and 2296. A Rogowski coil has been added in the diode as shown in Figure 11. Since there is no current neutralization in the diode, this monitor will give a reading of the primary diode current. Simultaneous measurements with this Rogowski coil and a large Faraday acting as the anode give the same results to within a few percent.

All diagnostics in the beam chamber are monitored with double-shielded RG-223/U cables with an additional shield slipped over and soldered directly to the BNC connectors.

b. Diode Impedance

Experiments were conducted on the DML to determine diode impedance as a function of anode-cathode (A-K) spacing for various shaped cathodes. The data soon showed, however, that the impedance changed continuously as a function of time. The application of Child's law,

$$Z = K V^{-\frac{1}{2}} \left(\frac{d^2}{r^2}\right) \Omega$$

where d is the anode-cathode spacing, r is the radius, and V is the voltage in megavolts, requires the K to take on values ranging from ≈ 130 down to ≈ 30, with an average K of ≈ 80. However, since the energy densities in the anode are high enough to vaporize the anode material, an attempt was made to interpret the impedance collapse data as an effect of the decrease in A-K gap during the pulse. Using the measured voltage waveform and a first order approximation to the anode velocity (a constant velocity of 1.5 cm/μsec commencing at t = 10 nsec), one can predict from Child's law (with K = 136) the impedance as a function of time. Comparison with the data in Figures 13 and 14 shows good correlation.

The first case considered is a 600 needle, 1¼ in. radius, slightly convex cathode (the needle points describe the surface of a 48 in. diam sphere). The impedance of this cathode set at 1.5-mm A-K is plotted in Figure 13 as a function of time for three different shots. The fact that the voltage across the diode was nearly identical for the shots allows plotting on the same graph. Using Child's law with K = 136 and an exploding anode yields the solid line. The V term was an average of the three shots at any instant in time.

The same analysis was then applied to a hollow cathode which was essentially the 600 needle convex but with the needles for R < 3/4 in. removed (see Figure 14). The r term used in Child's law was the geometric mean radius. Further refinements on the above calculation would require a better knowledge of the velocity of the anode plane. Specifically one must know the anode velocity as a function of time and radius for each of the cathodes studied.

c. Total Beam Energy

Diode impedance collapse mentioned previously leads to a very peaked behavior in the power curve at late times. Figure 15 is a

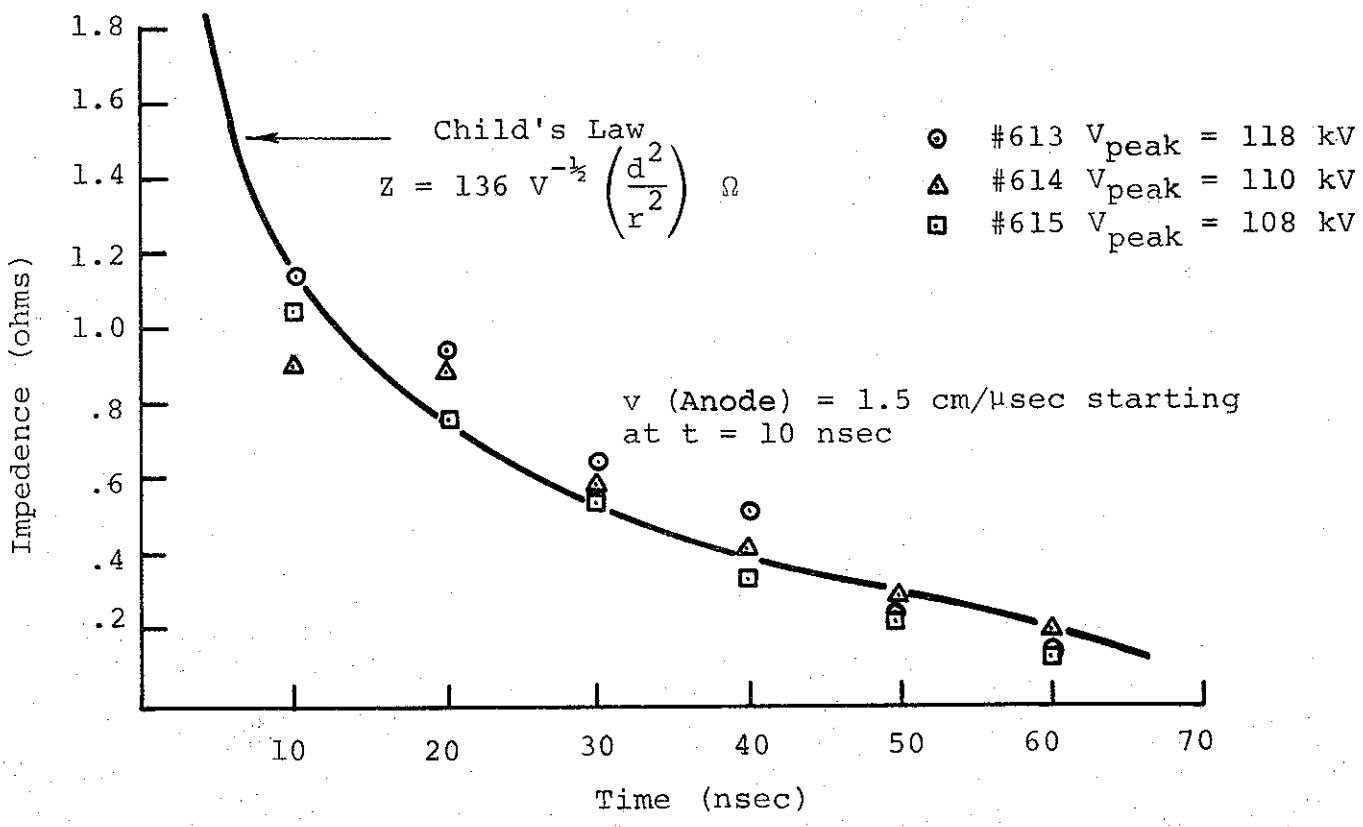

FIGURE 13. DIODE IMPEDENCE VS TIME FOR 600 NEEDLE 2-3/4-in. CONVEX CATHODE, 1.5-mm A-K

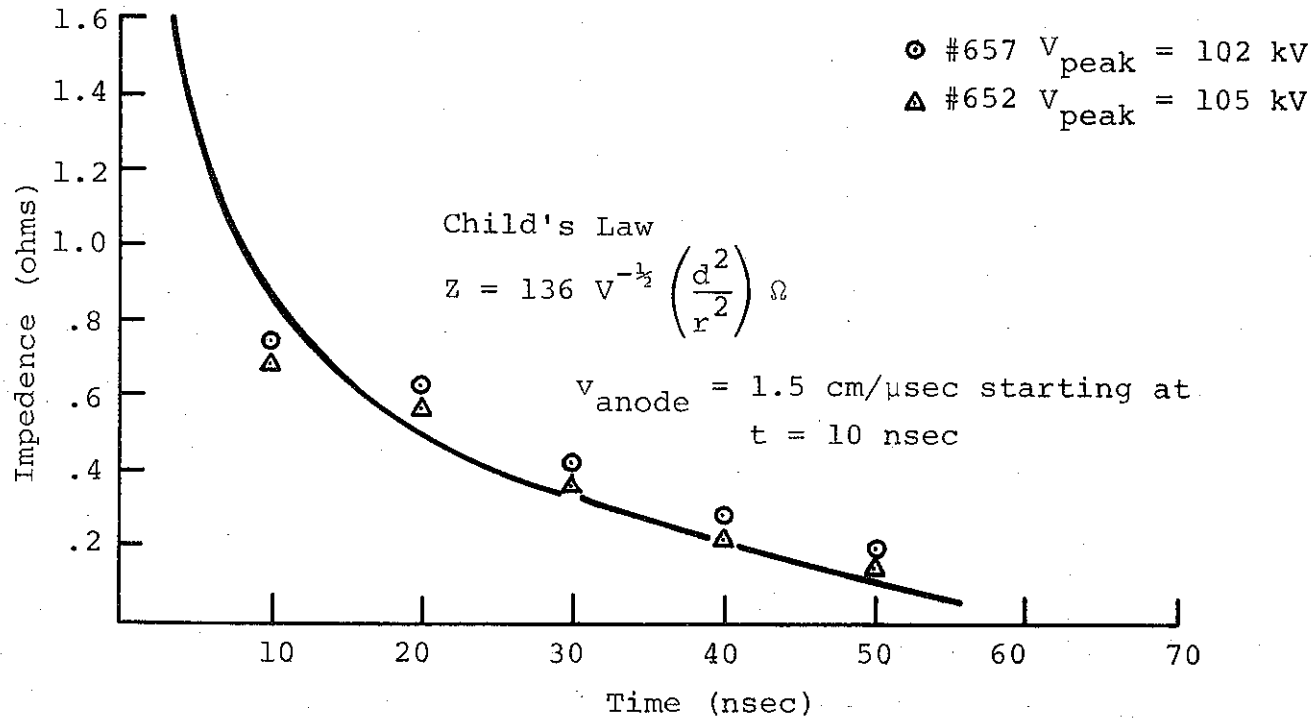

FIGURE 14. DIODE IMPEDENCE VS TIME FOR 2-3/4-in. O.D., 1-1/2-in. I.D. HOLLOW CATHODE, 1.0-mm A-K

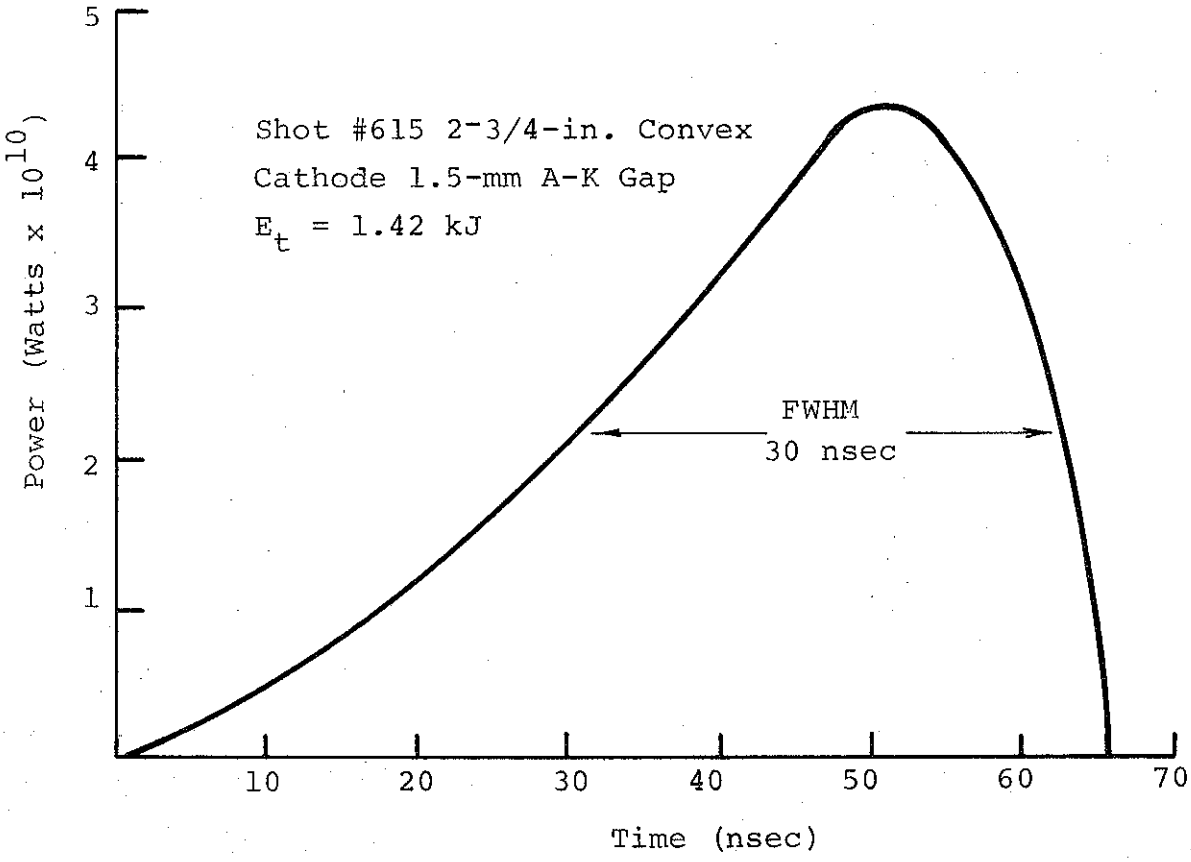

FIGURE 15. POWER VS TIME AT ANODE

plot of power transmitted to the anode at all times. Integration of the area beneath the curve gives a total energy transported to the anode of 1.42 kJ (340 calories).

d. Diode Pinching

Experiments are presently being made to determine current density as a function of time and position. The technique involves the use of a large Faraday cup as the anode over which are placed apertures of various sizes. By scaling the current read by the Faraday cup with that indicated by the diode Rogowski coil one can obtain the function $J(r,t)$ describing the beam.

The data are preliminary; however they do suggest that the beam does pinch in the diode but at late times in the pulse. If this is indeed true one may suggest that ions produced in the anode-cathode region may be required for the beam to pinch. Variation in prepulse conditions will be attempted to allow earlier beam collapse in the diode and a greater concentration of power density.

3. Linear Pinch Program

A linear pinch, or Z-pinch, has been constructed and thoroughly tested. The following sections will present construction details and the results of space- and time-resolved measurements of the magnetic field and current density of the discharge. Also included below are the results of space- and time-resolved measurements of the high ν/γ electron beam current density which will be injected into the Z-pinch in forthcoming experiments. The latter are described in the last section.

a. Construction of Z-Pinch Apparatus

Figure 16 schematically shows the elements of the apparatus. After the capacitor bank is dc-charged, the switch in the transmission line is closed and an electric field appears between the electrodes of the discharge tube. The pressure of the gas in the discharge tube is such that this electric field is sufficient to cause rapid avalanche breakdown of the gas. The capacitor bank then discharges through the LCR circuit consisting of the capacitor bank itself, the transmission line, and the gas discharge. The current-versus-time waveform is essentially that of a damped sinusoid, with perturbations in the first half-cycle due to inductance fluctuations associated with pinching of the discharge current (see Figure 17). Analysis of the current waveforms, obtained with the transmission line shorted, shows that the circuit, excluding the discharge tube, has $L = 62$ nH, $C = 42$ μF, $R = 6.3$ mΩ. The discharge tube adds from 20 to 100 nH, depending upon the stage of collapse of the discharge itself. Construction and circuit details follow.

1. Energy Source: Power Supply and Capacitor Bank

The dc-power supply is a standard unit capable of charging to 30 kV with current limited to < 3 mA. The charging resistor is 1 MΩ and electrically isolates the power supply from the rest of the apparatus. The capacitor bank consists of three 14 μF, low inductance (40 nH) capacitors, a total of 42 μF and 13.3 nH.

2. Transmission Line

The capacitor bank is connected across the discharge tube through a flat transmission line, 6 ft long and 10 in. wide. The sheets of the transmission line are 0.010-in. copper separated by 0.020-in. Mylar. The inductance of this transmission line is 5 nH.

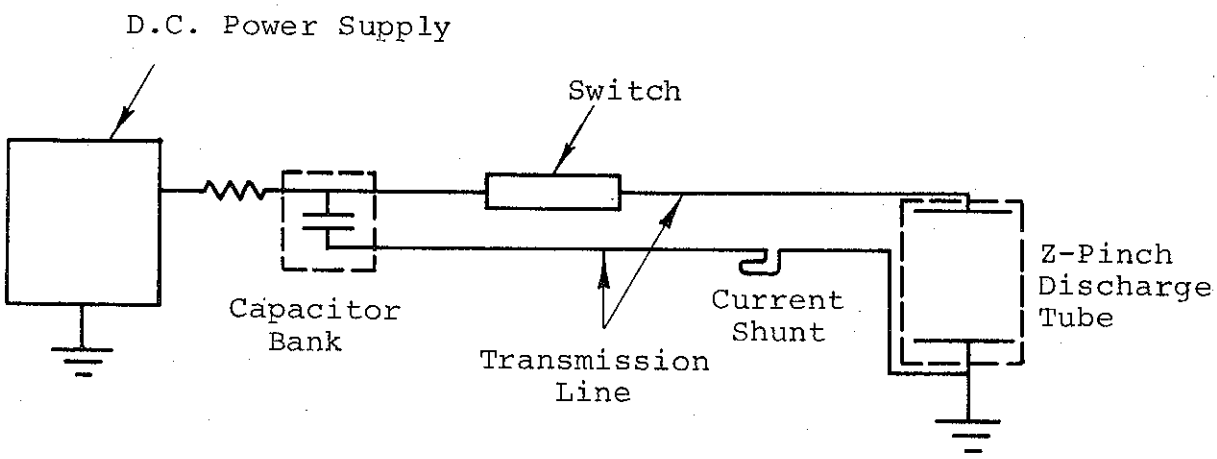

FIGURE 16. SCHEMATIC CIRCUITRY FOR Z-PINCH APPARATUS

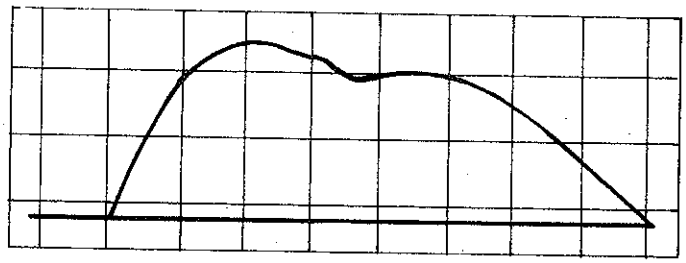

a

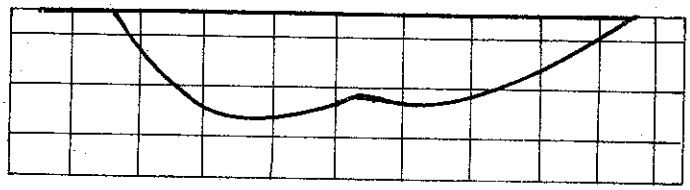

b

FIGURE 17. WAVEFORMS OBTAINED WITH THE 6kV, 500μ N_2 DISCHARGE: (a) ROGOWSKI COIL, 32.3 kA/cm, 1 μsec/cm; (b) CURRENT SHUNT, 52.2 kA/cm, 1 μsec/cm.

Inserted in the lower sheet of this line is a current shunt (see Figure 16) made of 0.001-in.-thick brass. The shunt has the same width as the transmission line (10 in.) and presents a resistance of 0.0014 Ω. It is used to monitor the total discharge current versus time. The shunt is folded once upon itself to provide a very low inductance path; Mylar insulation separates the folds.

3. Switch

The switch in the transmission line is a spark-gap switch consisting of two parallel brass rails (cylinders) and a knife edge between them. The external circuitry used to trigger the spark gap is shown in Figure 18. Circuit A uses a simple capacitor discharge to provide an 800 V, 1 μsec-wide spike to circuit B, a thyraton unit. The output of circuit B is a fast rise (≈ 50 nsec) 2500-V pulse. This fires the spark gap in circuit C by providing corona in the air between the two brass balls of that circuit. This, in turn, overvolts the gap in circuit D between the knife edge and one of the rails in the transmission line. When this gap fires, the remaining gap becomes overvolted and it, too, fires, completing the switch action. The time needed for all of this to occur is 300 nsec, with a jitter of about 50 nsec.

When the Z-pinch is fired in conjunction with an electron beam machine, circuit A will be replaced by a linkage with the trigger circuitry of the machine.

4. Discharge Tube and Diagnostics

The Z-pinch discharge apparatus and diagnostics are illustrated in Figure 19. Essentially this apparatus provides a low-inductance arrangement for connecting the transmission line to the flat electrodes of the discharge tube, which in the present configuration are 25-cm apart and 2 in. in diameter. The design shown in Figure 19

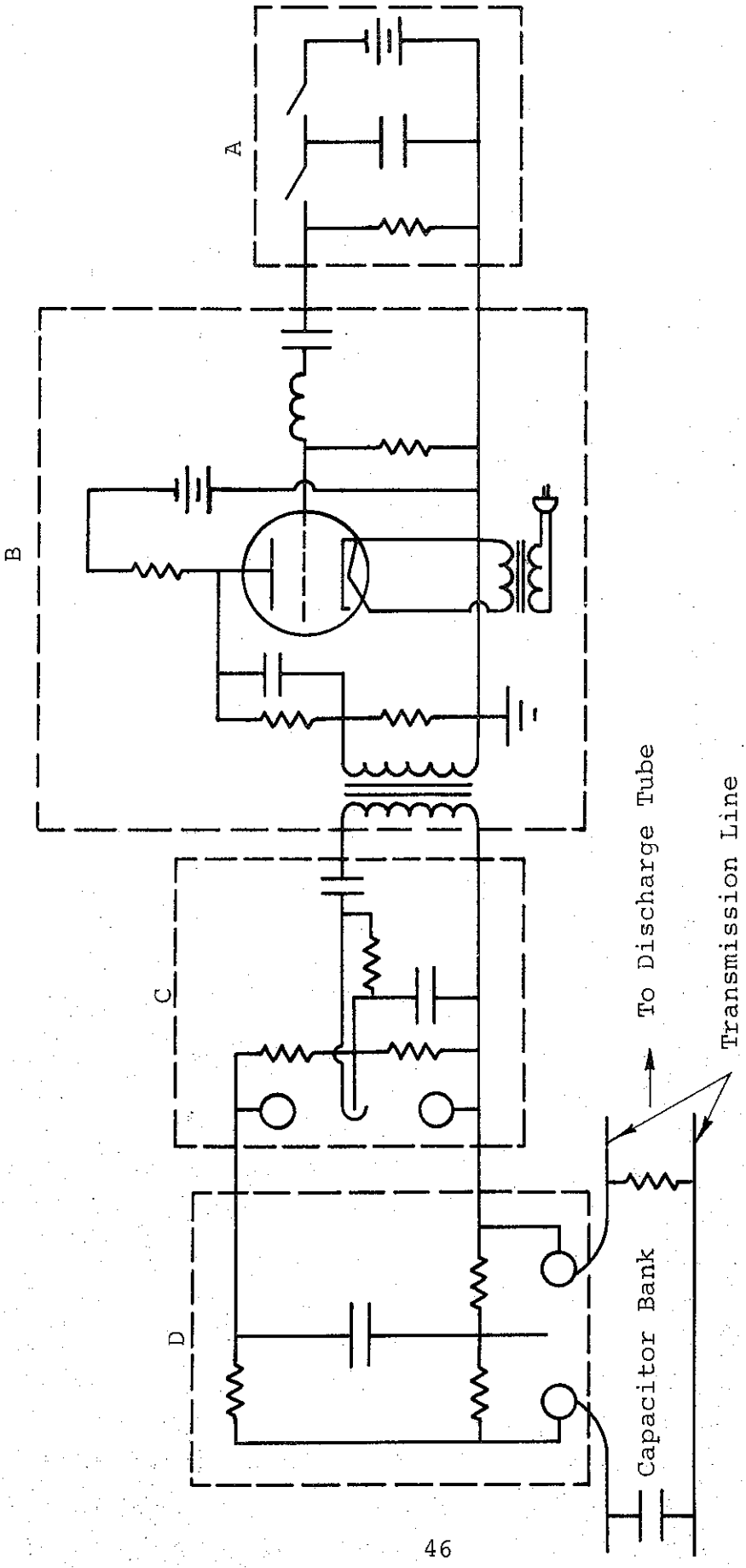

FIGURE 18. TRANSMISSION LINE SWITCH CIRCUITRY

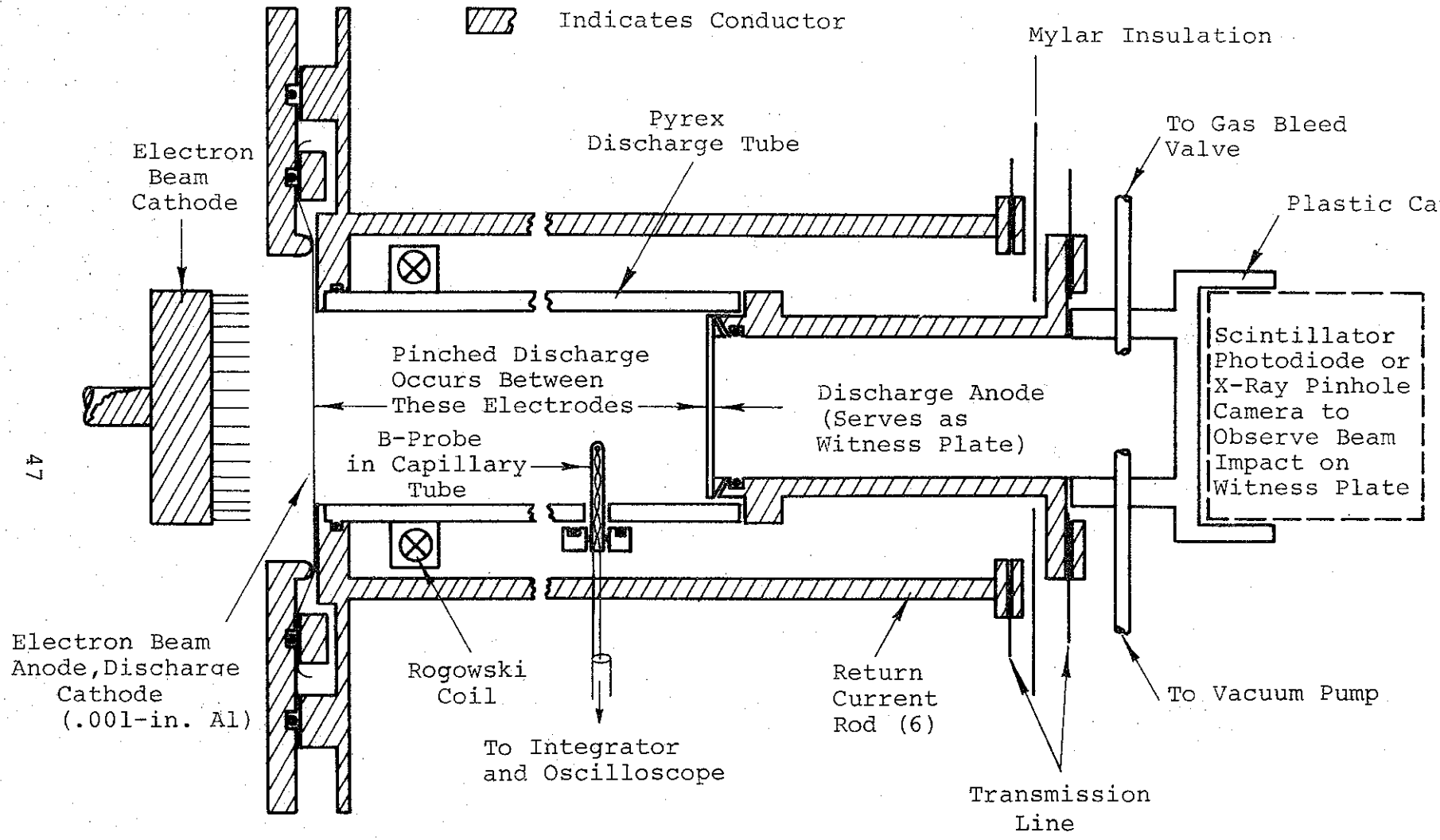

FIGURE 19. Z-PINCH DISCHARGE APPARATUS AND DIAGNOSTICS

makes it possible to change the length of the discharge by simply inserting a longer (or shorter) Pyrex discharge tube and longer (or shorter) return current rods.

A number of electrical and optical methods are used to measure the performance of the discharge.

The signal from the Rogowski coil (a helical loop enclosing the Pyrex discharge tube) is integrated at the oscilloscope by a standard RC-integrator circuit. This technique provides a total current-versus-time waveform that compares well with that obtained from the current shunt in the transmission line (Figure 17). Sensitivity of the Rogowski coil is 0.155 V/kA.

The B-probe is a very small coil (9 turns of 0.040 in. diam) oriented so as to intercept the azimuthal magnetic field, B_θ. The probe is contained in a quartz capillary tube inserted through a vacuum-sealed hole in the pyrex discharge tube. The signal from the probe is proportional to $\partial B_\theta/\partial t$ and is integrated at the oscilloscope by an RC-integrator circuit. By firing the discharge a number of times with the B-probe at a different radius each time, $B_\theta(r,t)$ is obtained. Using this field map, the longitudinal discharge current density $j_z(r,t)$ is calculated, as described in the next section.

In addition, the visible-light output of the discharge is monitored. This monitoring is done in three ways: open shutter (time-integrated) photography, time-resolved photography using a framing camera, and optical photodiode measurement of luminosity versus time at fixed radius.

Extensive measurements of discharges in both nitrogen and argon in the pressure range 10 to 1000 μ have been made. A discharge in argon at 500 μ, with the capacitor bank charged to 12 kV (corresponding to 3000 J of stored energy), has been selected for use in conjunction with the 738 Pulserad, 500 keV, 150 kA electron beam ($\nu/\gamma = 5.5$). This discharge was chosen on the basis of its appropriate current level (135 kA peak), its longitudinal stability and freedom from perturbing electrode end-effects, and the wide variety of current profiles available in the course of its time-history. Figure 20 shows total current and relative luminosity at the axis versus time for the 12 kV discharge in 500 μ argon. Figure 21 shows a time-integrated photograph of this discharge, and Figure 22 shows a sequence of framing camera photographs, ½-μsec apart. Magnetic field and current density data are presented in the next section.

In the electron-beam injection experiment only, the Rogowski coil, open-shutter photo, and current-shunt measurements will be made on the discharge, in addition to electron-beam diagnostics.

b. Z-Pinch B_θ and j_Z Maps

In the Z-pinch, a longitudinal electric field is applied to a cylinder of low-pressure gas and the ensuing breakdown rapidly ionizes the gas, creating a medium of high conductivity (≈ 100 mhos/cm). The increasing current at first flows primarily in a layer along the walls. When the magnetic pressure ($B_\theta^2/8\pi$) becomes sufficiently large and exceeds the gas pressure (nkt) the discharge collapses radially. One can note, in Figure 20, that the on-axis gas luminosity becomes appreciable, well after the discharge has begun. When this "pinch" reaches the axis, the plasma pressure rises and the motion is stopped and reversed.

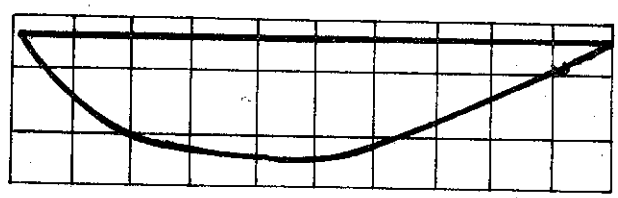

a

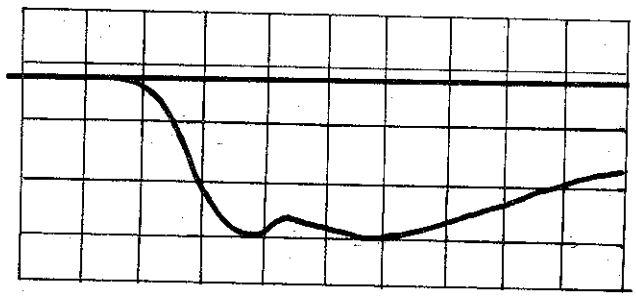

b

FIGURE 20. WAVEFORMS OBTAINED WITH THE 12kV, 500μ Ar DISCHARGE: (a) CURRENT SHUNT, 75 kA/cm, 1 μsec/cm; (b) PHOTODIODE (ON-AXIS), 1 μsec/cm. LUMINOSITY ON AXIS BECOMES APPRECIABLE AFTER 2 μsec; BEFORE THAT TIME THE CURRENT FLOWS MOSTLY AT LARGE RADII (SEE FIGURE 9).

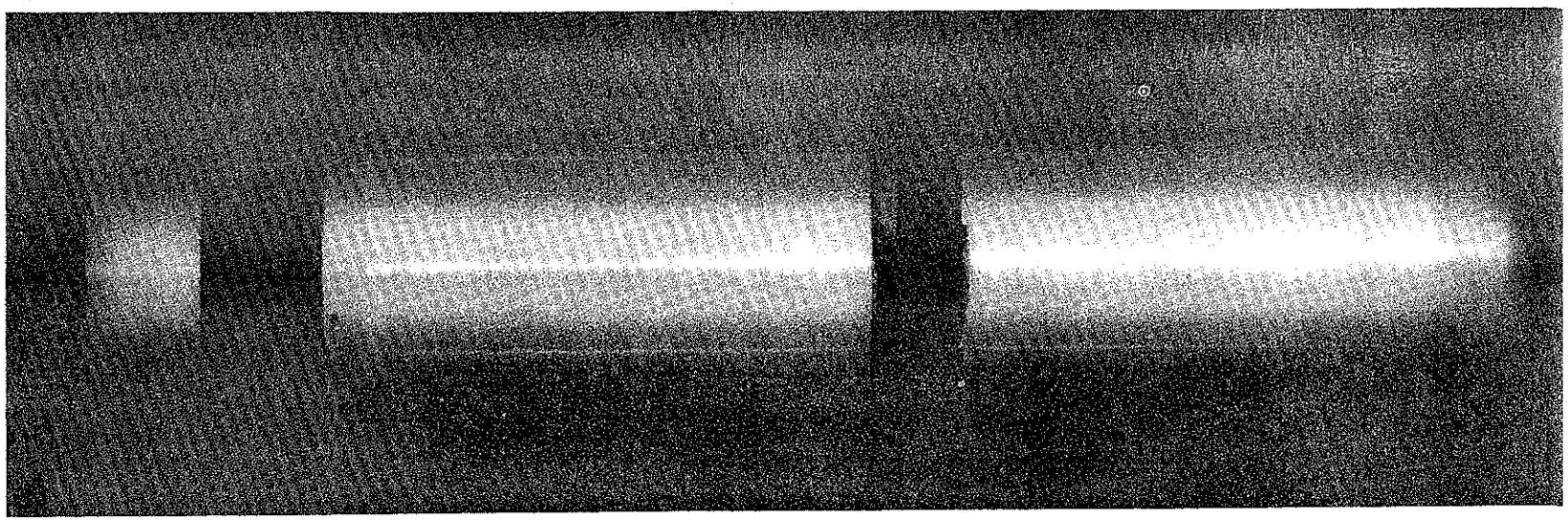

FIGURE 21. TIME-INTEGRATED (OPEN SHUTTER) PHOTOGRAPH OF 12 kV, 500 μ Ar DISCHARGE. DARK BANDS ARE B-PROBE VACUUM SEAL AND ROGOWSKI COIL.

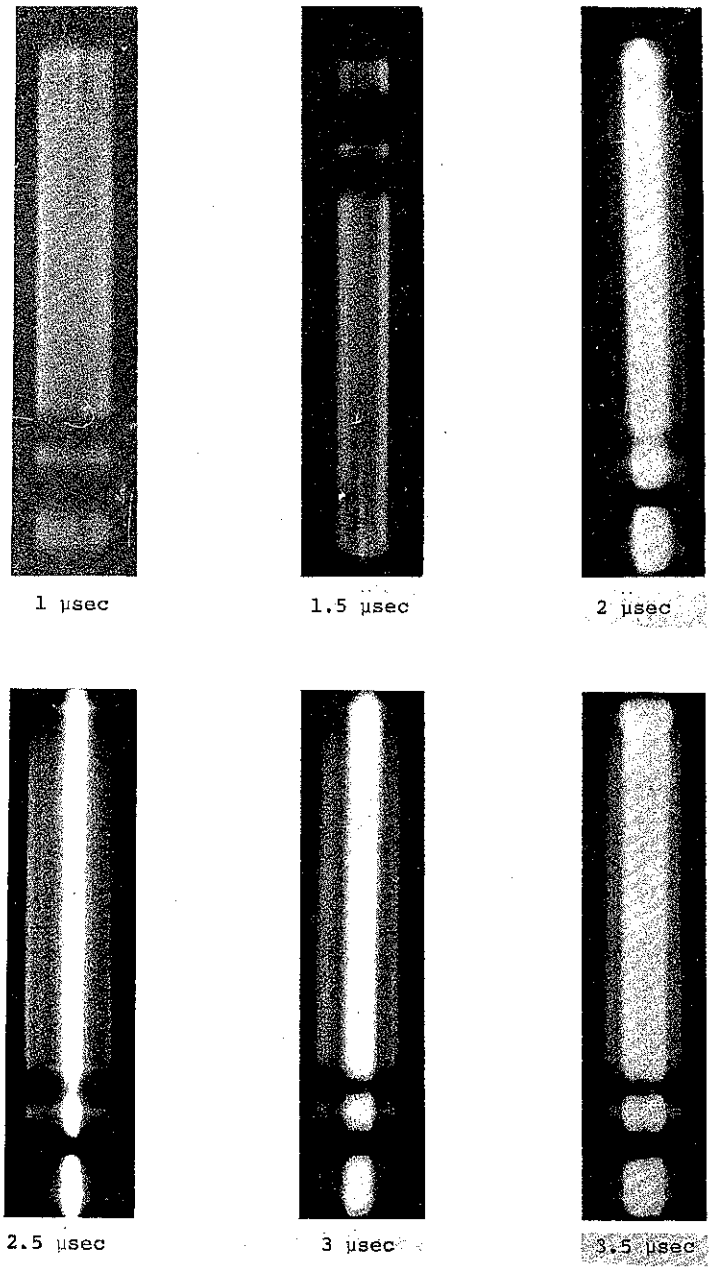

FIGURE 22. FRAMING CAMERA SEQUENCE OF 12 kV 500 µ ARGON DISCHARGE

The distribution of $B_\theta(r)$ for several times in the 12 kV, 500 μ, A discharge is shown in Figure 23. The axial current density is obtained from B_θ by Ampere's law:

$$j_Z(r) = \frac{c}{4\pi r} \frac{\partial}{\partial r} (r B_\theta) .$$

Current distributions are shown in Figure 24. These distributions clearly show the collapse of the pinch and the subsequent expansion. Maximum compression occurs at 2.5 μsec when I = 130 kA. Maximum current occurs at t = 4 μsec when I = 135 kA.

c. Electron-Beam Entrance Condition Measurements

Use of the Z-pinch described in the preceding three sections consists of injecting the electron beam concentrically into the active discharge (see needle cathode in Figure 3) at a known time. The time of injection determines the field and current profiles presented to the beam. It is felt that interpretation of the results of this experiment will require not only knowledge of the discharge current and field profiles, but a knowledge of the injected beam-current profile as well, $j_Z(r,t)$. For this reason an experiment was conducted with the 738 Pulserad in which a Faraday cup was used with a graphite aperture to measure total current flowing within a given radius at the anode plane. By taking a succession of such shots, with apertures having different diameters, the electron-beam current density at the anode plane can be calculated versus radius and time.

Figure 25 presents the results of this experiment performed using a slightly convex 600-needle cathode, 2½ in. in diam. The anode-cathode gap was set at 5 mm at the cathode edge, which yielded an electron beam having 500 keV mean energy and 150 kA peak current. This beam will be injected into each of the six discharge configurations shown in Figures 23 and 24. Further details of this forthcoming experiment are discussed in the next section.

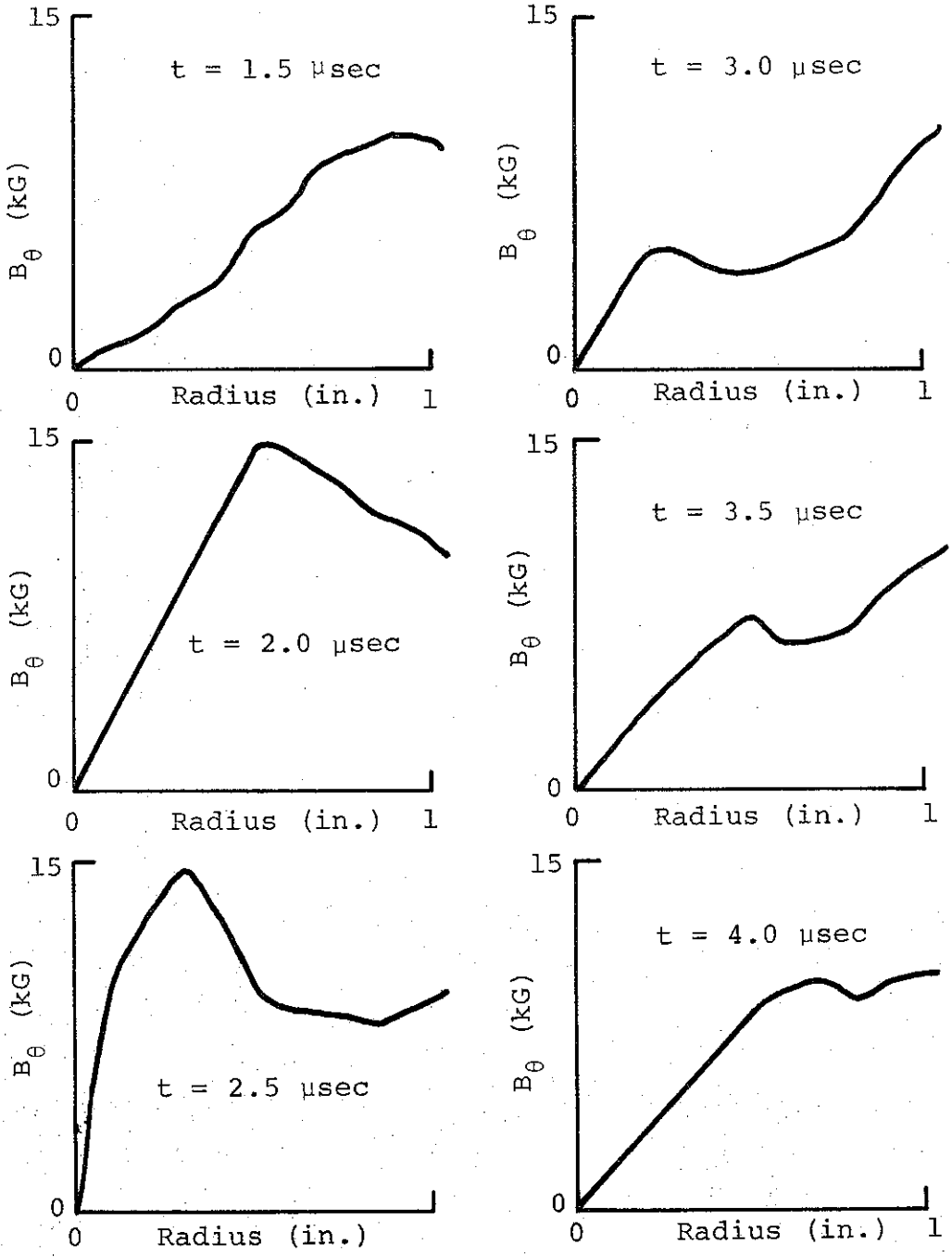

FIGURE 23. B_θ (r,t), 12 kV 500μ Ar DISCHARGE

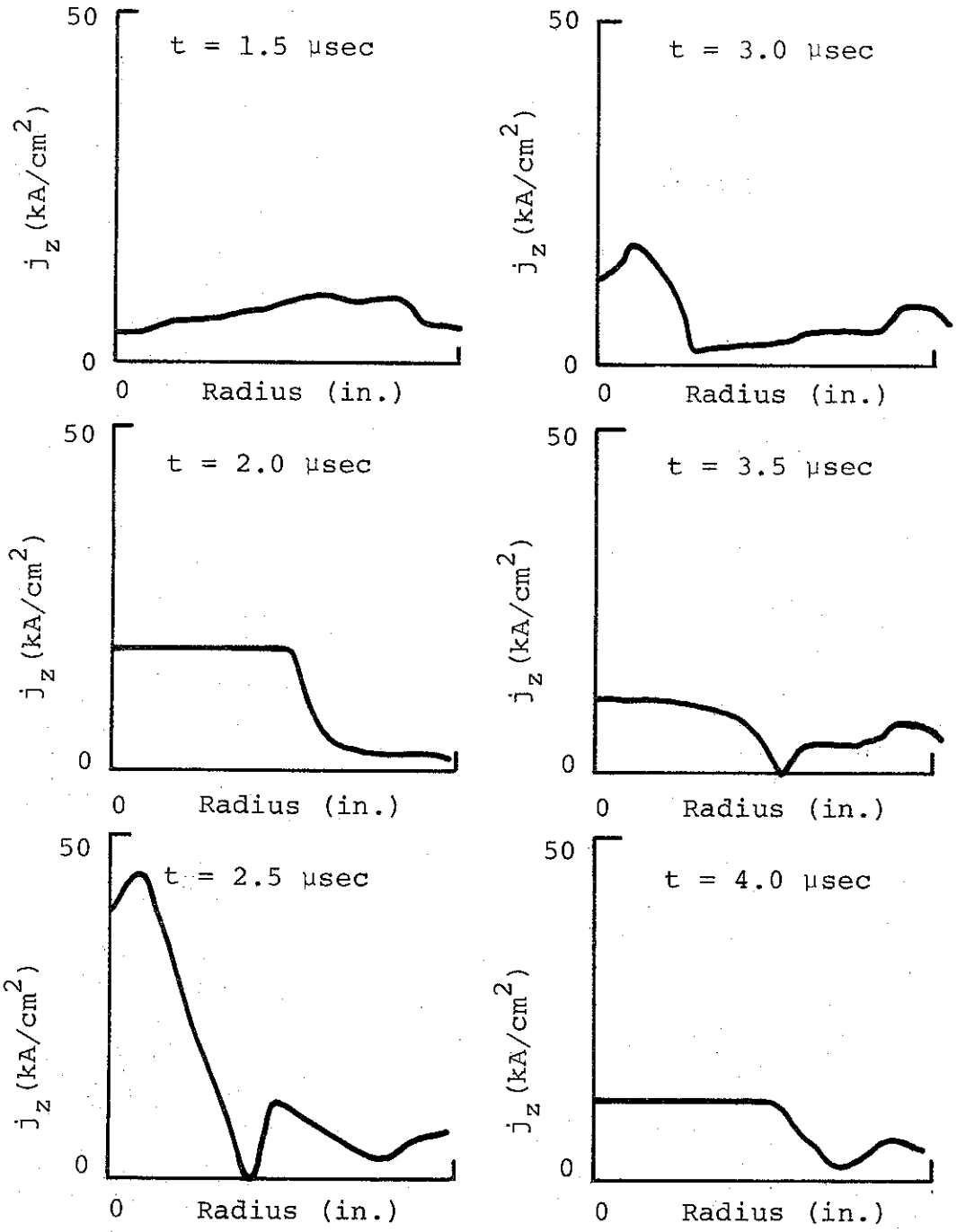

FIGURE 24. $j_z(r,t)$, 12 kV 500μ Ar DISCHARGE.

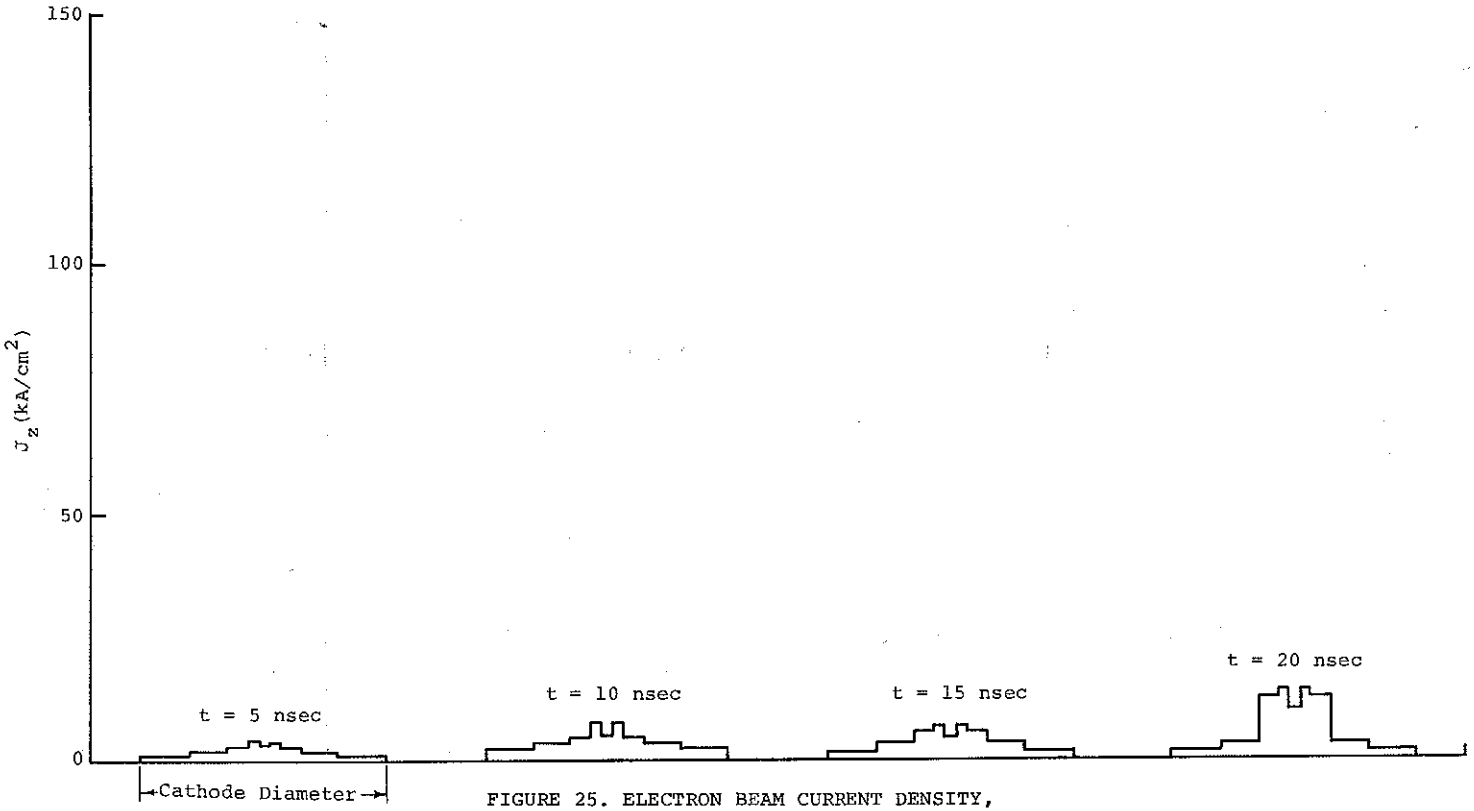

FIGURE 25. ELECTRON BEAM CURRENT DENSITY, $J_z(r, t)$, AT ANODE PLANE

R8890

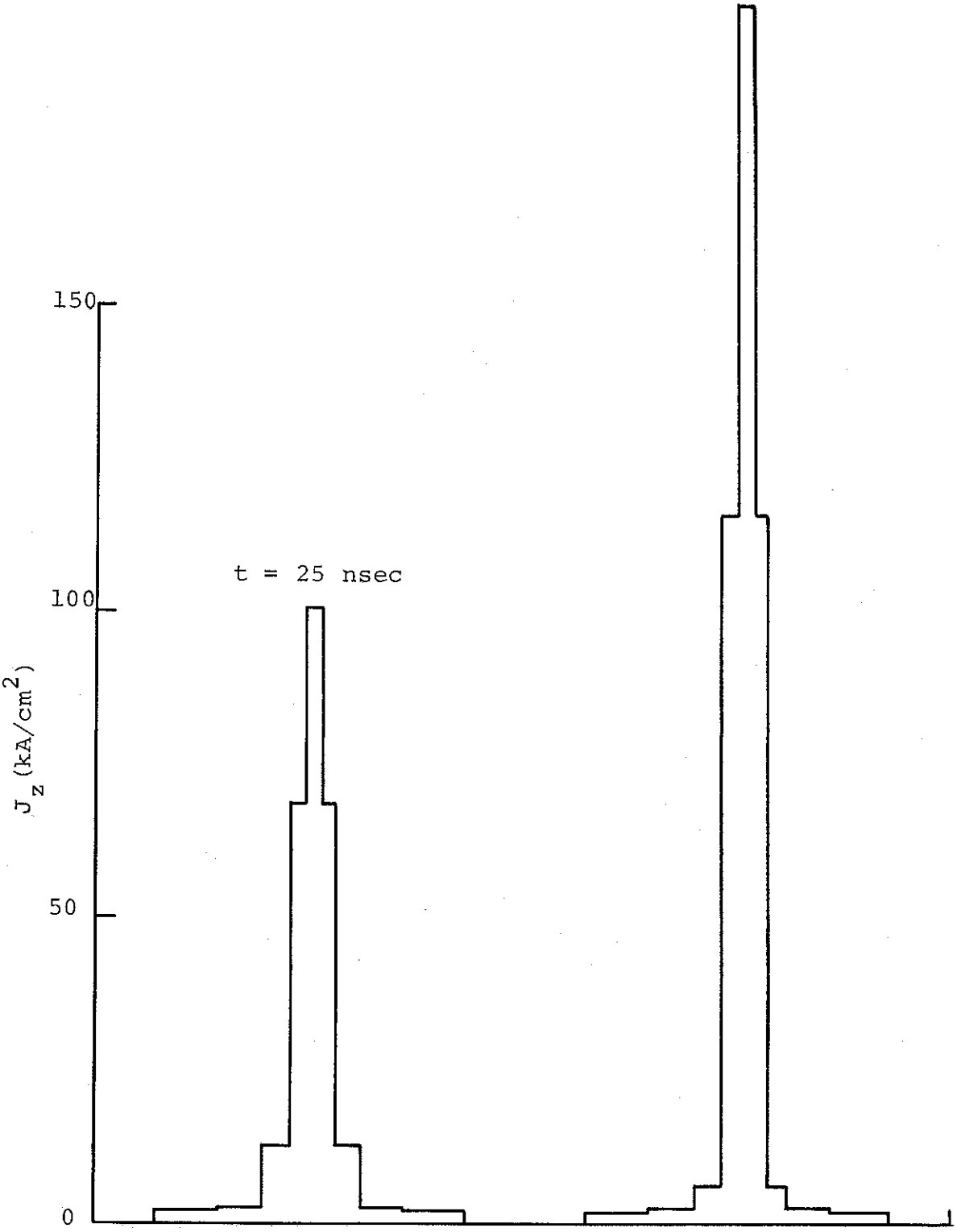

R8888

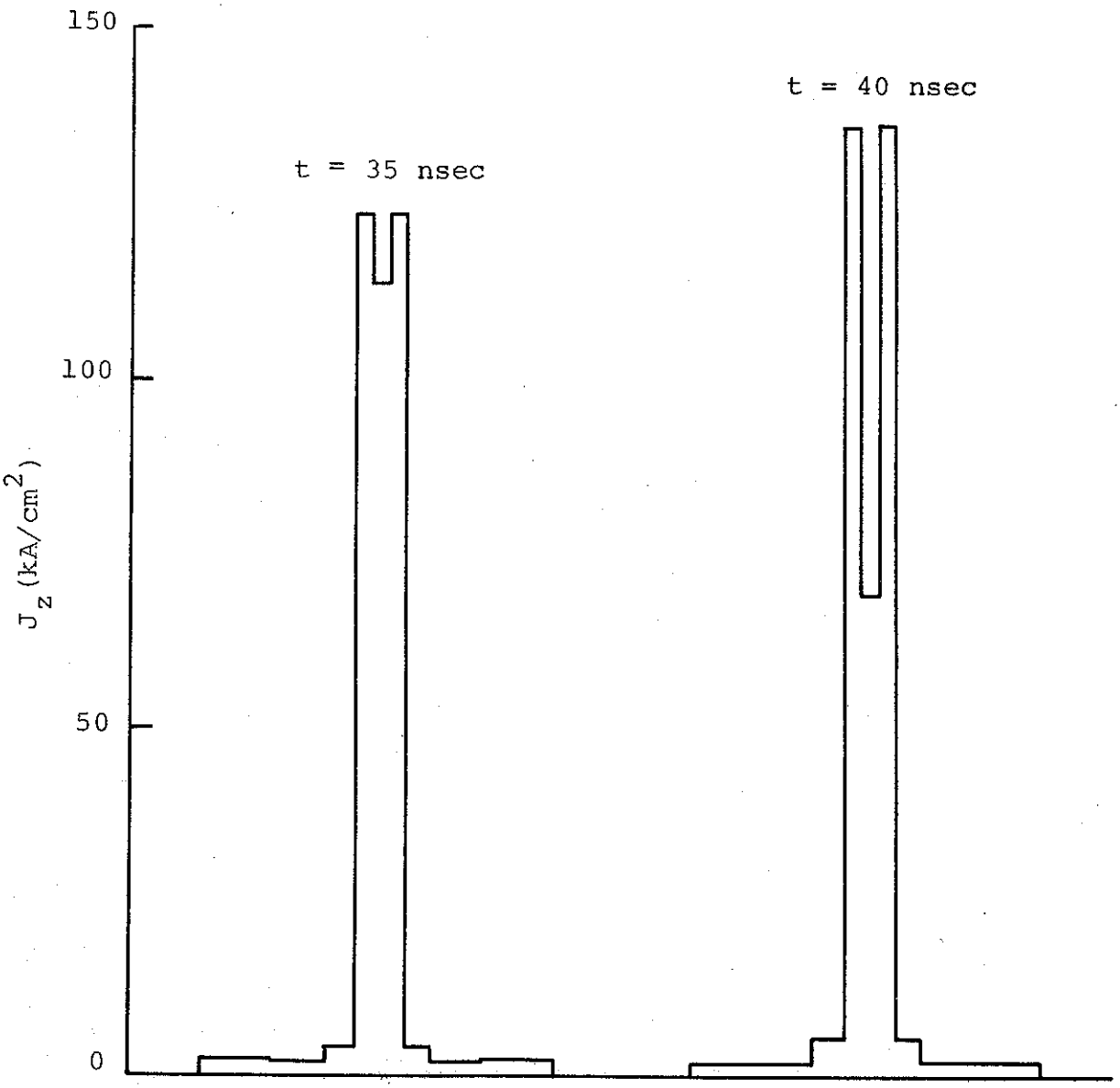

R8906

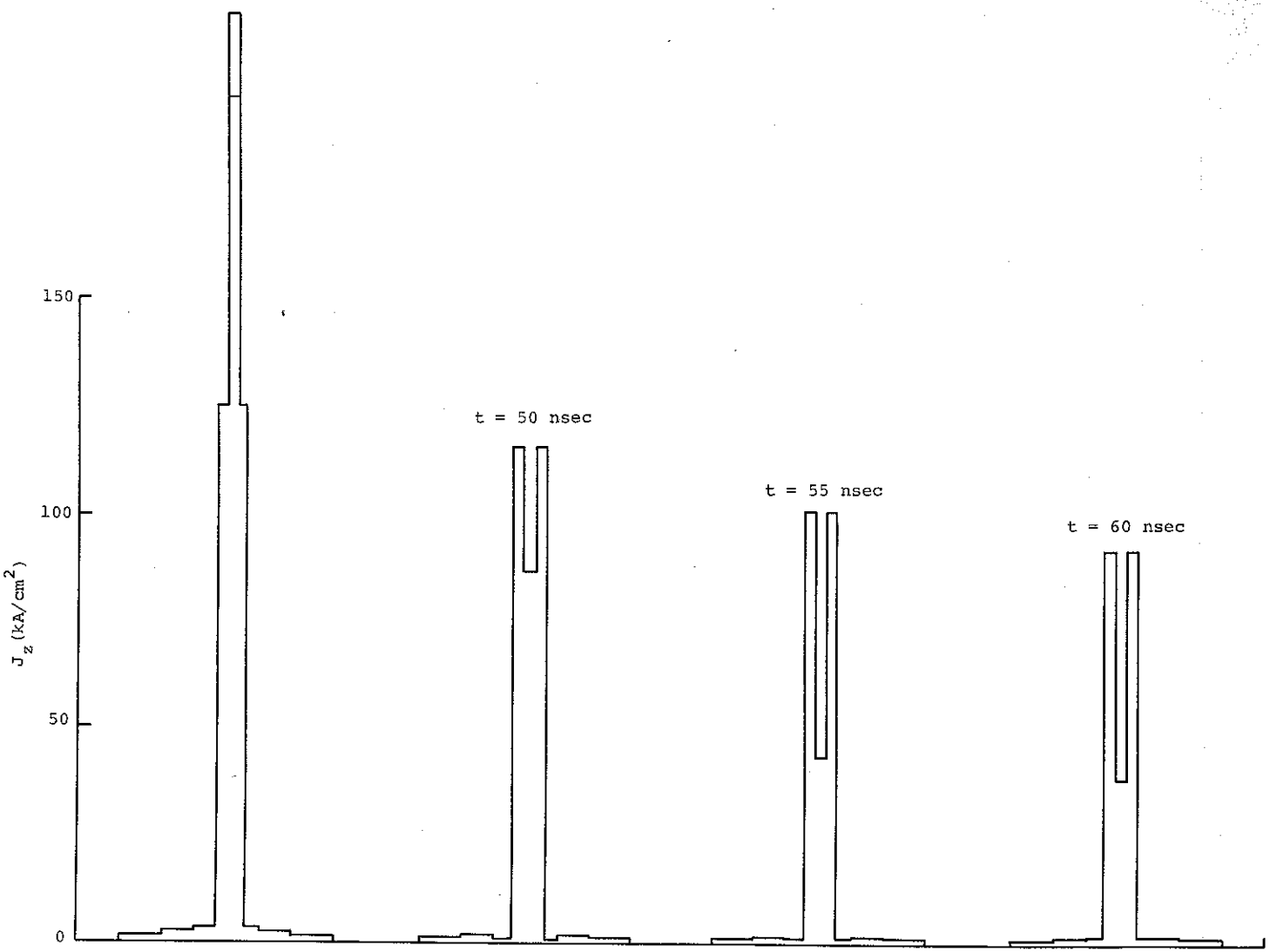

R8889

FIGURE 25. ELECTRON BEAM CURRENT DENSITY, $J_z(r, t)$, AT ANODE PLANE (CONT.)

d. Planned Experiments

The first experiment involving the injection of a high ν/γ electron beam into a Z-pinch will be performed shortly, utilizing the beam described in Section III and the discharge profiles shown in Figures 23 and 24.

Measurement of electron beam propagation will be made by observing X-ray production in the target, the high-voltage anode of the Z-pinch, a 2-in. aluminum disc 0.040 in. thick. The X-ray production will be observed with a scintillator-photodiode and with an X-ray pinhole camera on successive shots. For comparison, the same measurements of intensity and extent will be made with a target disk placed at the anode plane. Three fast Rogowski coils around the discharge tube at its ends and center will measure the extent of beam current neutralization. Correlation of scintillator-photodiode, Rogowski coil, and diode current signals will allow calculation of beam-front velocity in ionized and neutral cases. Additional information on propagation will be evident from damage sustained by the target and by the Pyrex discharge tube. Each of these will be replaced for every shot. Also, open-shutter photography of each injection will be done, and propagation of the beam in neutral gas (discharge not fired) will be measured as above for comparison.

Plans for further experiments are contingent upon results and interpretation of the initial efforts. If electron beam propagation along the pinch appears very efficient, a more rigorous test of propagation efficiency would consist of significantly increasing the length of the discharge.

SECTION IV

PROGRAM PLAN AND FINANCIAL STATUS

The following is a summary of the program plan for the period of March 30 to December 31, 1970.

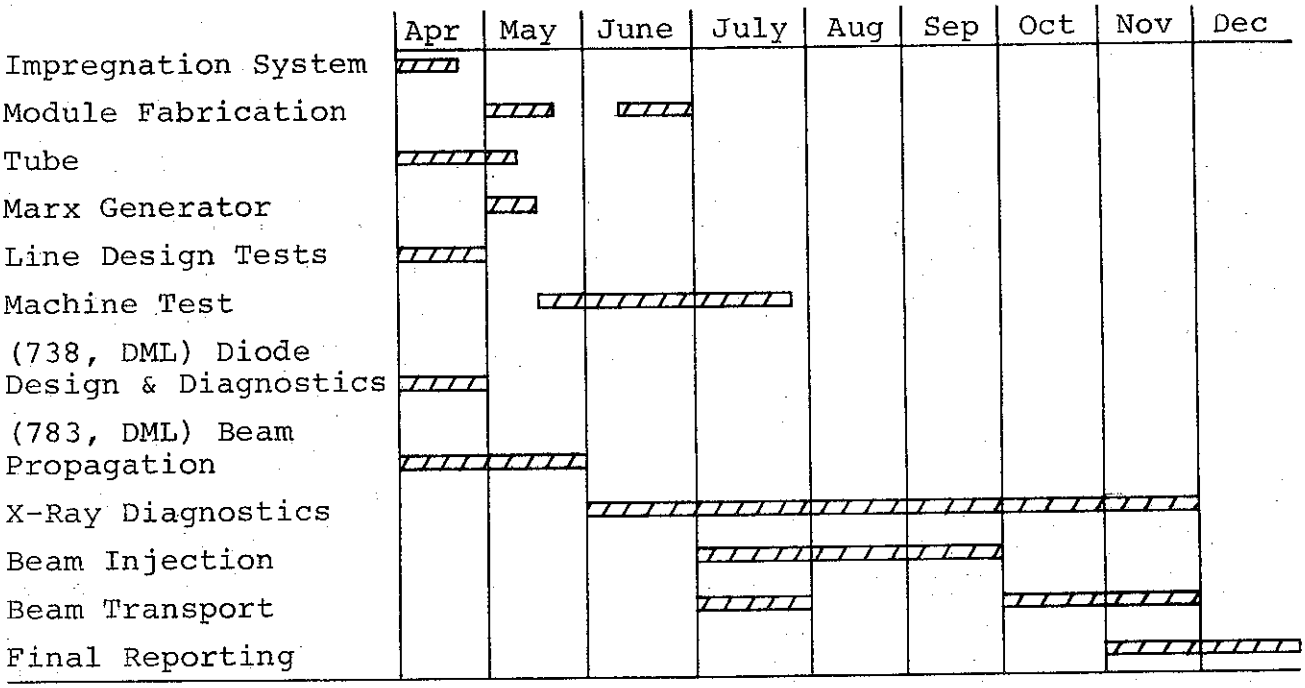

As can be seen from the schedule above, the first module will be finished in late May. At that time the Marx will also be finished, as will the tube. The line module will be tested into a resistive load and then into the tube. As soon as the first module is deemed acceptable, the second module will be constructed and both will be attached to the tube.

With this timing, a single module can be used to produce X-rays at full voltage but at only half the full current. This experiment will probably occur in late June. However, this single module will

not feed the tube symmetrically, may cause beam instabilities, and the results will have to be carefully interpreted. The first X-ray output with both modules is expected sometime in July.

Diode studies are currently being carried out using the 0.3 Ω low-impedance line (DML) and should be completed by the end of April. Beam transport experiments using a linear pinch apparatus have just begun and will continue on the 738 Pulserad and DML until the end of May. We expect to carry out preliminary X-ray diagnostics beginning with the first module in June and continuing throughout the remainder of the program. It is reasonable to expect that the dual module configuration will be fully operating and X-ray diagnostics well underway by October.

Diode and beam transport work will coincide with X-ray diagnostics from July until the end of November. Work on the final report will be started in November and submitted by January 1, 1971.

No unforseen difficulties have occurred in the program to date in so far as design or fabrication of hardware. Direct and labor costs have run at approximately the level proposed with the exception of the beam-propagation task, which has required labor expenditures at a greater rate than earlier anticipated. The next reporting period will be a better indication of the labor expenditure level required throughout the rest of the program in that the major design and purchasing tasks will have been completed and operational activities begun.